DOI: 10.1534/genetics.108.092155

Drosophila Nemo Promotes Eye Specification Directed by the Retinal Determination Gene Network

Lorena R. Braid and Esther M. Verheyen[1]

Department of Molecular Biology and Biochemistry, Simon Fraser University, Burnaby, British Columbia V5A 1S6, Canada

Manuscript received June 2, 2008
Accepted for publication July 15, 2008

ABSTRACT

Drosophila *nemo* (*nmo*) is the founding member of the Nemo-like kinase (Nlk) family of serine–threonine kinases. Previous work has characterized *nmo*'s role in planar cell polarity during ommatidial patterning. Here we examine an earlier role for *nmo* in eye formation through interactions with the retinal determination gene network (RDGN). *nmo* is dynamically expressed in second and third instar eye imaginal discs, suggesting additional roles in patterning of the eyes, ocelli, and antennae. We utilized genetic approaches to investigate Nmo's role in determining eye fate. *nmo* genetically interacts with the retinal determination factors Eyeless (Ey), Eyes Absent (Eya), and Dachshund (Dac). Loss of *nmo* rescues *ey* and *eya* mutant phenotypes, and heterozygosity for *eya* modifies the *nmo* eye phenotype. Reducing *nmo* also rescues small-eye defects induced by misexpression of *ey* and *eya* in early eye development. *nmo* can potentiate RDGN-mediated eye formation in ectopic eye induction assays. Moreover, elevated Nmo alone can respecify presumptive head cells to an eye fate by inducing ectopic expression of *dac* and *eya*. Together, our genetic analyses reveal that *nmo* promotes normal and ectopic eye development directed by the RDGN.

THE adult structures of *Drosophila melanogaster* are patterned during the larval stages in discrete epithelial compartments called imaginal discs. Larval imaginal discs are inherited from the embryo as small groups of progenitor cells (Garcia-Bellido and Merriam 1969). As these cells proliferate, each imaginal disc becomes compartmentalized into fields of cells expressing unique protein sets. Each protein set confers a specific cellular identity. As development progresses, highly complex and integrated signaling networks further refine the fields of cells to achieve the final organ pattern. These signaling networks not only orchestrate cell determination, but also tightly regulate proliferation and cell survival to ensure the proportionality of the resulting adult.

In Drosophila, the adult eyes, antennae, and the majority of head structures are derived from the eye-antennal imaginal discs (Haynie and Bryant 1986). The smaller, anterior region of the disc is fated to become the antenna, and the larger posterior compartment contains the eye and head primordia. In this article, we refer to the anterior and posterior compartments as the antennal and eye discs, respectively (Figure 1B). These discs are composed of two epithelial layers: the main epithelium (ME) and the squamous peripodial epithelium (PE) (Haynie and Bryant 1986). The ME comprises primordia of the compound eye, its surrounding cuticle, and the antennae, while the PE gives rise to the remainder of the head. Studies have revealed a novel role for PE cells in directing cellular events in the ME through cell–cell signaling mediated by lumenal processes (Gibson and Schubiger 2001).

Eye specification is directed in the posterior region of the eye disc by the concerted efforts of the retinal determination gene network (RDGN), a cassette of evolutionarily conserved nuclear factors (Figure 1A; reviewed in Pappu and Mardon 2004; Silver and Rebay 2005; Jemc and Rebay 2006). RDGN mutants are generally characterized by loss of eye tissue (Bonini *et al.* 1993; Cheyette *et al.* 1994; Mardon *et al.* 1994; Quiring *et al.* 1994). *twin-of-eyeless* (*toy*) (Czerny *et al.* 1999) and *eyeless* (*ey*) (Quiring *et al.* 1994) are *Pax-6* genes positioned at the top of the network hierarchy. *toy* is expressed in the embryonic eye field and activates *ey* in all cells of the first instar larval imaginal disc (Figure 1A) (Czerny *et al.* 1999). The primary eye/antennal division of the disc is achieved by downregulation of *ey* in the anterior-most region of the disc in early second instar, allowing expression of the antennal selector *cut* (Kenyon *et al.* 2003). Ey deploys the RDGN by activating *sine oculis* (*so*) and *eyes absent* (*eya*) expression at the posterior margin (Halder *et al.* 1998; Kenyon *et al.* 2003). So is a member of the Six family of homedomain transcription factors (Cheyette *et al.* 1994). *eya* encodes a novel nuclear protein with protein tyrosine phosphatase and transactivating activity (Bonini *et al.* 1993; Rayapureddi *et al.* 2003; Silver *et al.* 2003; Tootle *et al.* 2003). Eya complexes with a variety of cofactors, including So (Pignoni *et al.* 1997) and Dachshund (Dac) (Chen *et al.*

[1]*Corresponding author:* Simon Fraser University, 8888 University Dr., Burnaby, BC V5A 1S6, Canada. E-mail: everheye@sfu.ca

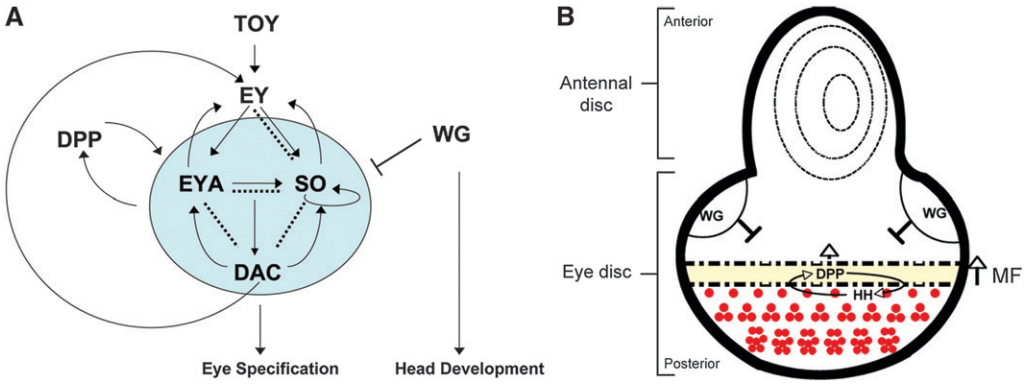

Figure 1.—The retinal determination gene network. (A) Regulatory interactions within the RDGN. Solid arrows show direct transcriptional regulation, curved arrows demonstrate feedback loops, and dashed lines indicate physical interactions. So, Eya, and Dac are not required for *ey* expression during normal eye development, but can activate its expression in ectopic eye assays (Pignoni *et al.* 1997). Modified from Pappu and Mardon (2004) and Silver and Rebay (2005). (B) Schematic of a third instar eye-antennal imaginal disc. The antennal disc gives rise to the antenna and surrounding head cuticle. In the eye disc, the MF marks the dynamic boundary between the posterior, differentiated eye cells and the anterior head primordia. Hh activates *dpp* transcription in the furrow, which promotes expression of the RD genes and drives the MF forward. Wg, secreted from the anterior dorsal and ventral lobes, promotes head specification by inhibiting furrow progression and transcription of retinal specification genes. Anterior is up; dorsal is left.

1997), to regulate a battery of transcriptional targets. Dac is a nuclear protein required for furrow initiation and ommatidial patterning (Mardon *et al.* 1994). Dpp is required for expression of *eya*, *so*, and *dac* during the second larval instar (Curtiss and Mlodzik 2000; Kenyon *et al.* 2003) and early third instar (Chen *et al.* 1999). So and Eya subsequently maintain *dpp* expression, thereby forming a positive feedback loop (Pignoni *et al.* 1997; Hazelett *et al.* 1998).

Patterning of the retinal field occurs in the posterior region of the third instar eye disc (Figure 1B). The diffusible morphogens Wg and Dpp act antagonistically to promote head and eye fates, respectively (Royet and Finkelstein 1997). The retinal determination (RD) genes *so*, *eya*, and *dac* are key factors in this mutual antagonism. At the onset of third instar, *hh* alleviates *dpp* repression along the posterior margin (Royet and Finkelstein 1997; Pappu *et al.* 2003). Dpp antagonizes *wg* (Wiersdorff *et al.* 1996; Chanut and Heberlein 1997; Pignoni and Zipursky 1997; Royet and Finkelstein 1997), allowing initiation and subsequent progression of the morphogenetic furrow (MF) (Dominguez and Hafen 1997; Pignoni and Zipursky 1997). The MF sweeps across the eye disc in a posterior-to-anterior direction, conferring neural identity through induction of *atonal* (*ato*) (Jarman *et al.* 1994, 1995; Zhang *et al.* 2006). As the furrow traverses the disc, expression of the RD genes *so*, *eya*, and *dac* is maintained in its wake, as well as in the cells immediately anterior to it (Cheyette *et al.* 1994; Curtiss and Mlodzik 2000; Bessa *et al.* 2002; Pappu *et al.* 2003). Wg signaling in the anterior head primordia represses *so*, *eya*, and *dac* transcription (Baonza and Freeman 2002).

A prevalent theme in morphogenesis is the spatial and temporal regulation of specific cofactors to achieve differential interactions and outcomes using common factors. Such combinatorial control is exemplified by the RDGN. Although Ey initiates expression of *so*, *eya*, and *dac* during the second instar, it is restricted to cells anterior to the furrow during the third instar (Halder *et al.* 1998) where it promotes Wg activity to inhibit furrow progression (Bessa *et al.* 2002). In cells immediately anterior to the furrow, and thus receiving high levels of Dpp, Ey activates *eya* expression to repress the Wg target *homothorax* (*hth*) (Bessa *et al.* 2002). Cells more anterior receive a higher dose of Wg than Dpp and are still actively proliferating and adopting head fates. Here Ey complexes with Hth and another Wg effector, Teashirt (Tsh), to repress *eya* transcription, effectively inhibiting the RDGN and eye determination (Bessa *et al.* 2002). Thus, Ey can function as both a retinal selector and antagonist depending on its cellular context, an environment specified by the set of available cofactors.

Drosophila *nemo* (*nmo*) was first identified as a gene required for ommatidial rotation during establishment of planar cell polarity during eye development (Choi and Benzer 1994). *nmo* is the founding member of the Nemo-like kinase (Nlk) family of proline-directed serine–threonine kinases (Choi and Benzer 1994). Nlks are highly conserved from worms to mammals and play diverse roles in regulating cell signaling throughout development (Ishitani *et al.* 1999; Rocheleau *et al.* 1999; Zeng *et al.* 2007). Phosphorylation by Nlks has been shown to affect the activity of a number of proteins, including Tcf/Lef family members (Ishitani *et al.* 1999; Rocheleau *et al.* 1999) and the Drosophila Smad1 ortholog Mad (Zeng *et al.* 2007). *nmo* is an essential gene and loss of both maternal and zygotic *nmo* results in embryonic lethality (Mirkovic *et al.* 2002). *nmo* loss-of-function alleles survive to adulthood through perdurance of maternally supplied gene product and manifest numerous tissue patterning and growth defects (Choi and Benzer 1994; Verheyen *et al.* 2001; Zeng and Verheyen 2004; Zeng *et al.* 2007). *nmo* compound eyes have a distinct

morphology; compared to wild type, *nmo* eyes are long and narrow and display square, rather than hexagonal, packing of ommatidial clusters (Choi and Benzer 1994). In addition to rotation defects, *nmo* mutants have reduced capacity to specify ommatidia, resulting in smaller eyes (Fiehler and Wolff 2008).

In this study we describe a dynamic pattern of expression for *nmo* that suggests that it may have previously uncharacterized roles in early division of eye-antennal disc, in eye specification, and in patterning the ocellar region and antennae. We show that *nmo* is co-expressed with various combinations of the retinal determination genes in the eye disc beginning in the second larval instar during specification of the eye field. Later, *nmo* not only is expressed within and behind the MF (Choi and Benzer 1994), but also is ubiquitously expressed in the PE, in the presumptive ocelli, and in a discrete pattern in the antennal disc. Loss of *nmo* modifies *ey* and *eya* mutant phenotypes, suggesting that *nmo* may modulate development mediated by the RDGN. In ectopic eye induction assays, reducing endogenous Nmo represses this effect, suggesting a requirement for *nmo* in RDGN-mediated fate respecification. Furthermore, Nmo potentiates the ability of Ey, Eya, and Dac to respecify head, wing, and leg tissue to retinal fate. Sufficiently high levels of Nmo induce anterior head-to-eye transformations. These respecified cells show altered transcription of the same genes affected in RD-induced ectopic eyes, supporting a role for Nmo in promoting RDGN activity. Our clonal analysis demonstrates that Nmo does not modify transcription of the canonical RD genes, further suggesting that Nmo may affect output from the RD selector complexes. Reducing endogenous *nmo* also rescues small-eye defects induced by early misexpression of *ey* and *eya*. Moreover, directed co-expression of *nmo* and *ey* or *eya* in this assay severely disrupts eye and head formation, revealing a potent synergy. Together, our data implicate *nmo* as a positive mediator of RDGN activity in the imaginal eye disc.

MATERIALS AND METHODS

Fly genetics: All crosses were performed at 25° unless otherwise stated. The following fly strains were used: nmo^{P}, also referred to as *nmo-lacZ* (Choi and Benzer 1994; Zeng and Verheyen 2004), nmo^{adk1} and nmo^{adk2}, which express truncated transcripts (Verheyen *et al.* 1996, 2001), nmo^{DB24}, a molecular null (Zeng and Verheyen 2004), ey^{R}, ci^{1} (Quiring *et al.* 1994), eya^{2} (Zimmerman *et al.* 2000), dac^{1}/CyO (Mardon *et al.* 1994), dac^{E462}, *FRT40/CyO, dpp-lacZ* (Blackman *et al.* 1991), *so-lacZ* (Cheyette *et al.* 1994, provided by U. Waldorf), and *ey-lacZ* (provided by U. Waldorf). Misexpression analyses were performed using *UAS-nmo*$^{C5\text{-}1e}$ and *UAS-nmo*^{b27} (Verheyen *et al.* 2001), *UAS-GFP::nmoII* (provided by R. Fiehler, Fiehler and Wolff 2008), *dpp-Gal4* (Staehling-Hampton *et al.* 1994), *ey-Gal4* (Hazelett *et al.* 1998), *UAS-ey* (Halder *et al.* 1995), *UAS-dac*^{21M5M4}(kindly provided by G. Mardon), and *UAS-eya*^{1} and *UAS-eya*^{2} (Bonini *et al.* 1998). To examine pharate lethal phenotypes, animals were dissected from pupal cases.

Clonal analysis: *nmo* somatic clones were induced using the FLP/FRT method (Xu and Rubin 1993). To induce *nmo* loss-of-function clones using *hs-FLP,* embryos from the appropriate crosses were collected for 24 hr and the hatched larvae were heat-shocked at 38° for 90 min at 48 hr of development. The genotypes examined for β-galactosidase staining of *dpp-lacZ* in nmo^{DB24} and nmo^{adk2} clones were *dpp-lacZ/ey-FLP; nmo FRT 79D/Ubi-GFP FRT79D*, or *y hs-FLP22/+*; *dpp-lacZ/+*; *nmoFRT 79D/Ubi-GFP FRT79D*; for β-galactosidase staining of *so-lacZ* in nmo^{DB24} and nmo^{adk2} clones, *so-lacZ/ey-FLP; nmo FRT 79D/Ubi-GFP FRT79D* or *y hs-FLP22/+*; *so-lacZ/+*; *nmo FRT 79D/Ubi-GFP FRT79D*; for β-galactosidase staining of *ey-lacZ* in nmo^{DB24} and nmo^{adk2} clones, *ey-lacZ/ey-FLP; nmo FRT 79D/Ubi-GFP FRT79D* or *y hs-FLP22/+*; *ey-lacZ/+*; *nmo FRT 79D/Ubi-GFP FRT79D*; for all other antibodies, nmo^{DB24}, nmo^{adk1}, nmo^{adk2}, and nmo^{P} alleles were used in the following scheme: *ey-FLP/+; nmo FRT 79D/Ubi-GFP FRT79D* or *y hs-FLP22*; +; *nmo FRT 79D/Ubi-GFP FRT79D*. nmo^{DB24} somatic clone images in Figure 10 were generated using *ey-FLP.*

dac^{E462} somatic clones were induced in nmo^{DB24} and nmo^{adk1} heterozygotes in the following genotype: *y hs-FLP22*; dac^{E462}, *FRT40/ Ubi-GFP, FRT40*; *nmo/+*.

Immunostaining: Dissection of imaginal discs and antibody staining was performed following standard protocols. The antibodies used were rabbit anti-Atonal (1:1000; gift of Y. N. Jan, Jarman *et al.* 1994), mouse anti-β-galactosidase (1:500; Promega), rabbit anti β-galactosidase (1:2000; Cappel), mouse anti-β-galactosidase (1:250, Promega), mouse anti-cyclin B [1:20; Developmental Studies Hybridoma Bank (DSHB)], mouse anti-Dac$^{2\text{-}3}$ (1:75; DSHB), mouse anti-Eya^{10H6} (1:200; DSHB), rabbit anti-Ey (1:1000, gift of U. Walldorf, Halder *et al.* 1998), rat anti-ELAV (1:100; DSHB), mouse anti-Glass (1:2; DSHB), guinea pig anti-Hth (1:1000, gift of R. Mann, Abu-Shaar *et al.* 1999), rabbit anti-Hth (1:500, gift of G. Morata, Azpiazu and Morata 2002), and rabbit antiphospho-histone 3 (1:1000, Upstate Biotechnology). Secondary antibodies were used at 1:200 and obtained from Jackson Immunolabs and Molecular Probes.

Microscopy: Imaginal disc images were acquired with Improvision OpenLab Version 5.0.2 software using a QImaging RETIGA EXi camera mounted to a Zeiss Axioplan 2 microscope unless otherwise stated. Confocal images in Figure 3, H and J, and Figure 8, E–H, were acquired on an inverted Zeiss LSM410 laser-scanning microscope. All images were processed in Adobe Photoshop 6.0.

Adult flies were preserved in 95% ethanol and photographed using an EOS Rebel 300D digital camera mounted to a Leica MZ6 stereomicroscope. Images were processed in Helicon Focus and Adobe Photoshop 6.0.

RESULTS

***nmo* is expressed dynamically throughout imaginal eye-antennal disc development:** Analysis of *nmo* in the eye imaginal disc to date has focused solely on its third instar expression within and posterior to the MF (Choi and Benzer 1994). We have previously described expression of *nmo* in the wing disc, which is broadly initiated during second instar and is subsequently refined in the third instar (Zeng and Verheyen 2004). Given its dynamic temporal expression during wing development, we considered that *nmo* may also be expressed in the early eye-antennal imaginal disc. Using the nmo^{P} lacZ strain as a reporter for *nmo* transcription (Choi and Benzer 1994; Verheyen *et al.* 2001), we carefully characterized the expression pattern during larval eye development.

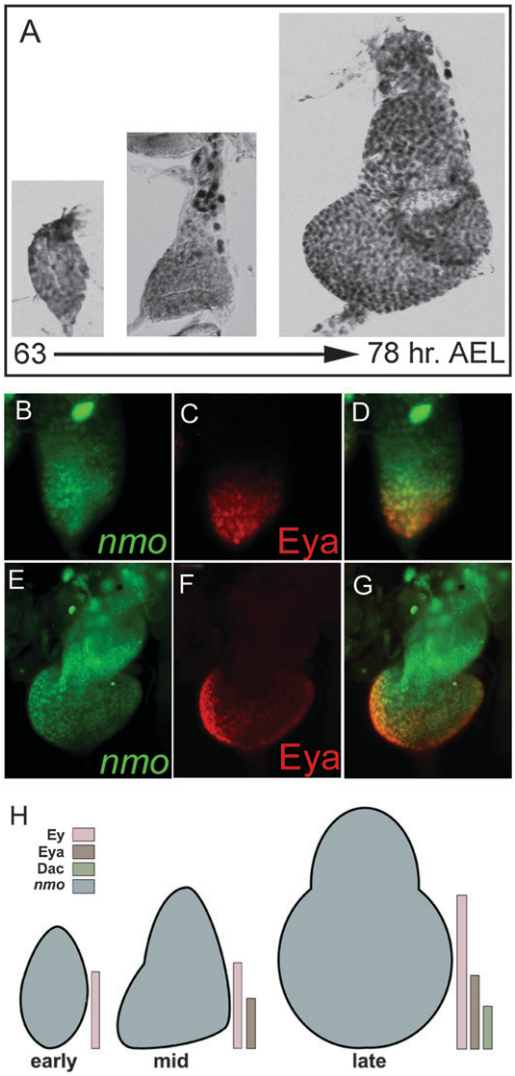

Figure 2.—*nmo* is co-expressed with the RDGN in the second instar eye disc. Expression of the *nmo-lacZ* enhancer trap during second instar eye disc development [63–72 hr after egg laying (AEL)], detected with anti-β-gal antibody. (A) *nmo-lacZ* is expressed in all cells. (B–G) *nmo-lacZ* (green, B and E) coincides with Eya (red, C and F) in the posterior eye disc in mid (B–D) and late (E–G) second instar. (H) Schematic summarizing *nmo*'s co-expression with the eye-specification genes. Early: *nmo* and Ey are co-expressed in the posterior eye field. Mid: *nmo* is co-expressed with Ey in anterior cells of the eye field and with Ey and Eya in posterior cells. Late: same is in mid, except at the posterior margin where *nmo* is co-expressed with Ey, Eya, and Dac.

We found that *nmo* is expressed ubiquitously in the peripodial cells of the second instar eye imaginal disc (Figure 2A), suggesting that Nmo may have an earlier, uncharacterized role in patterning the eye and head. *nmo* expression coincides with Eya in the posterior eye disc in mid- (Figure 2, B–D) and late (Figure 2, E–G) second instar. During second instar, the eye-antennal imaginal disc is segregated into antennal and eye territories through downregulation of *ey* in the anterior antennal region (Kenyon *et al.* 2003). Ey subsequently deploys the retinal determination network in posterior cells, resulting in increasing refinement of *eya* and *dac* expression to the posterior margin of the eye disc (Halder *et al.* 1998; Kenyon *et al.* 2003). Thus, *nmo* is co-expressed with different combinations of RD factors in a spatially and temporally regulated manner when the eye territory is initially established (Figure 2H).

As the third larval instar progresses, *nmo* is expressed in discrete subsets of cells. Posterior co-expression of *nmo* and Eya in second instar now extends to the anterior edge of the MF (Figure 3, A–C, arrow), but does not extend into the anterior pre-pro-neural (PPN) domain occupied by Eya and Dac (Figure 3, D–F, bracket in F). In late third instar discs, *nmo* expression is detected in the ocellar primordia. This expression is completely coincident with Eya (Figure 3, A–C, arrowhead) and more refined than Dac, which is more broadly expressed in the dorsal vertex primordia (Figure 3, E and F, arrowhead). Notably, the Wg target Hth is repressed in the ocellar cells co-expressing *nmo* and Eya (Figure 3, H and I, arrowhead in I). At the posterior margin, *nmo-lacZ* is repressed in cells expressing Hth (Figure 3I) and Ey (data not shown; Bessa *et al.* 2002). In the antennal disc, *nmo* expression is found in the aristal and Johnston's organ progenitors, according to the fate map of Haynie and Bryant (1986). Here, *nmo* is co-expressed with the pro-neural factor Ato (Figure 3, J–L). Ubiquitous peripodial expression of *nmo* persists during the third instar as *nmo* is expressed in all cells of the PE (Figure 3M), coincident with Hth (Figure 3N) and Ey (data not shown; Bessa *et al.* 2002).

This dynamic pattern of co-expression led us to hypothesize that *nmo* may contribute to multiple patterning events in the eye-antennal disc, in addition to its characterized role in planar polarity. Consistent with its expression in the ocellar primordia, *nmo* mutants display defects in the dorsal vertex (L. R. Braid, unpublished results). The antennae of *nmo* mutants appear normal, but given its co-expression with the neuronal marker *ato*, more refined analysis may uncover subtle sensory organ defects. *nmo*'s dynamic spatial and temporal co-expression with the eye-specification factors also suggested that it may contribute to early patterning of the eye and antennal fields. In this study, we focused our investigation of *nmo*'s potential novel roles in eye and head development to determine its function in eye specification, specifically by evaluating its ability to modulate the transcription and/or activity of the RDGN.

***nmo* rescues the *ey* small-eye phenotype:** We generated *nmo*; *ey* double mutants, using the *nmo* alleles nmo^{DB24}, nmo^{adk1}, nmo^{adk2}, and nmo^{P} to test whether *nmo* contributes to RD-mediated eye patterning. Homozygous *nmo* mutants display narrow eyes and ommatidial rotation defects (Figure 4B; Choi and Benzer 1994). We chose to perform our loss-of-function analysis using the severe hypomorph $ey^{Russian}$ (ey^{R}) (Quiring *et al.* 1994), which phenocopies the rare square ommatidial

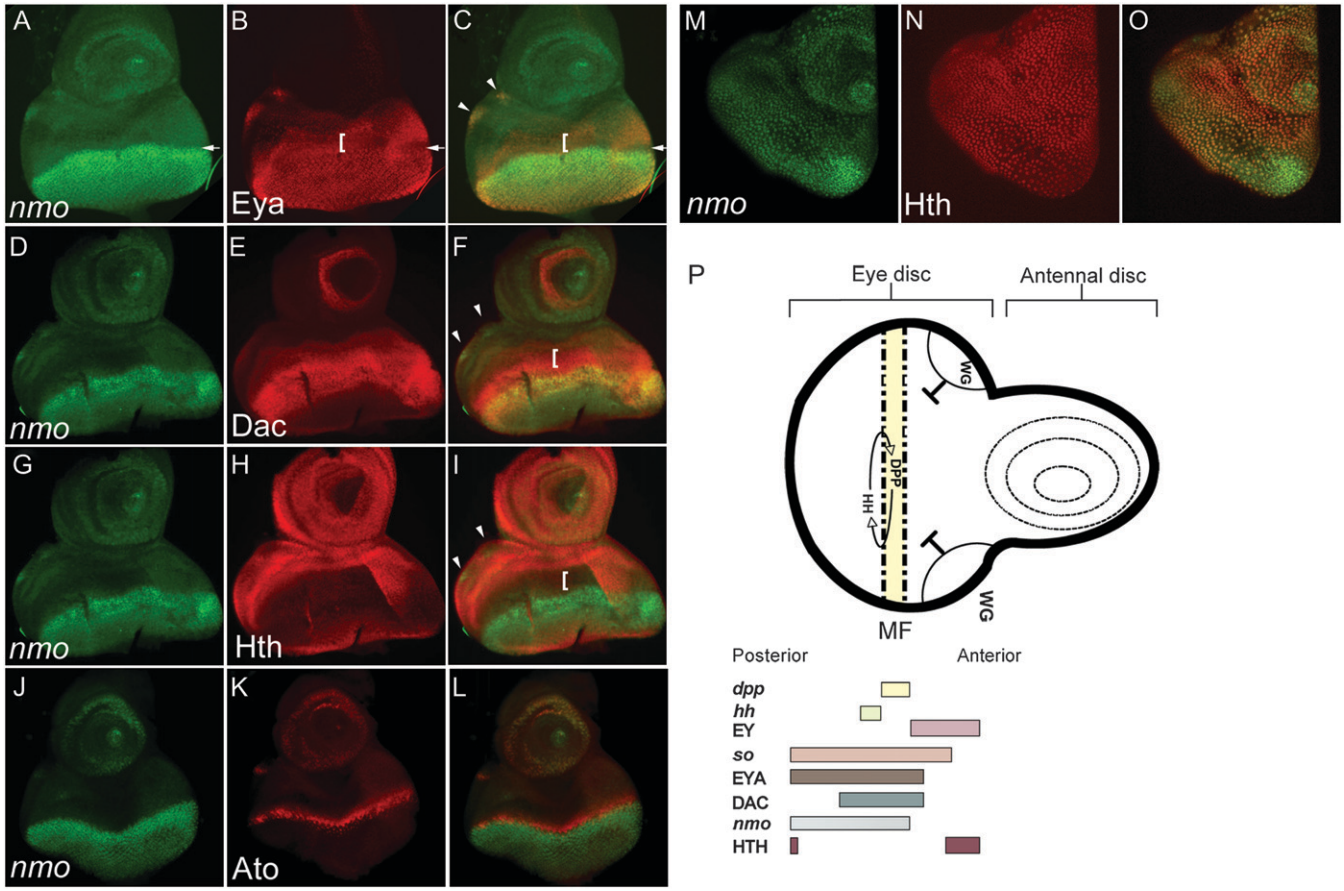

Figure 3.—*nmo* is expressed in multiple cellular contexts in the third instar eye-antennal disc (late third instar:140 hr AEL). All discs are oriented with dorsal left, anterior up. (A–C) *nmo-lacZ* (green) is coincident with Eya (red) in the MF (arrow) and in the ocellar progenitors (arrowheads) and, to a lesser degree, posterior to the furrow. *nmo-lacZ* is absent in the PPN domain (bracket). (D–F) *nmo-lacZ* (green) coincides with Dac (red) in the third antennal disc segment, in addition to the MF and retinal cells. *nmo-lacZ* overlaps with Dac in the presumptive ocelli (arrowheads in F), although Dac more broadly encompasses the entire dorsal vertex region. (G–I) Hth (red) is absent in eye disc cells expressing *nmo-lacZ* (red) and reduced in the ocellar primordia (arrowheads in I). (J–L) *nmo-lacZ* (green) is coincident with Ato (red) in the MF, the ocellar region, and the antennal disc. (M–O) Single confocal section. *nmo-lacZ* (green) (M) and Hth (red) (N) are expressed in all cells of the PE. (P) Schematic of a third instar eye/antennal disc. The regions of *dpp* and *wg* expression and their action on MF progression are shown. The MF moves posterior to anterior. *nmo*'s expression relative to the RD genes and the Wg effector Hth in the eye disc are indicated below, as previously described (Bessa *et al.* 2002; Silver and Rebay 2005).

array characteristic of *nmo* mutants (Hartman and Hayes 1971; Ready *et al.* 1976). *ey* mutants display variable loss of eye and head tissue (Figure 4C) as a result of large-scale apoptosis early in the third instar (Halder *et al.* 1998). Flies heterozygous for *nmo* or ey^R appear normal (data not shown). *nmo*/+; ey^R/+ flies displayed slightly smaller eyes (Figure 4D). Heterozygosity for ey^R did not significantly modify any aspect of the homozygous *nmo* eye phenotype (Figure 4E).

Loss of *nmo* did, however, rescue several aspects of the ey^R mutant eye, indicating that Nmo may contribute to some aspects of Ey-mediated eye development. *nmo*; ey^R double mutants had larger eyes than ey^R mutants alone (Figure 4F), as the number of ventral ommatidia was increased. ey^R mutants frequently display duplicated ventral vibrissae, the set of sensory bristles surrounding the ventral eye margin (Figure 4C, arrowhead). Loss of *nmo* rescues the bristle duplication to a normal single set (Figure 4F, arrowhead). In addition, the periphery of *nmo*; ey^R compound eyes are restored to wild type, being uniform compared to the irregular eye/head boundary typical of ey^R mutants (compare Figure 4, C and F). Interestingly, eyes of *nmo*;ey^R double mutants retained the narrow A–P width characteristic of *nmo* mutants, although the overall eye is smaller (compare Figure 4, B and F).

nmo and *ey* are co-expressed in the entire eye disc during second instar (Figure 2), in the third instar PE, and in the ocellar primordia of the ME (Figure 3). *nmo* is also co-expressed with the eye-specification genes *so*, *eya*, and *dac* during second instar within the furrow itself and the photoreceptor field behind it and in the presumptive ocelli (Figures 2 and 3). We therefore investigated whether *nmo* also genetically interacts with RD factors downstream of Ey.

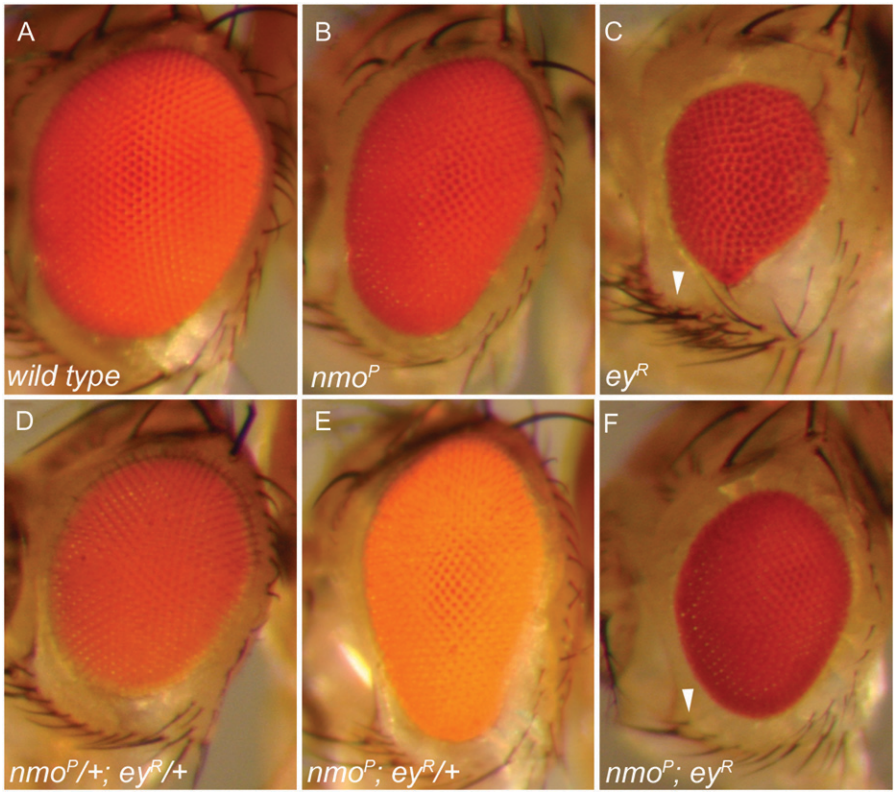

FIGURE 4.—*nmo* modifies the *ey* small-eye phenotype. (A) Wild-type compound eye. (B) nmo^{P} mutants have narrow eyes and a square ommatidial array. (C) ey^{R} compound eyes are small with disorganized ommatidia and uneven eye margins. The ventral row of sensory vibrissae is often duplicated (arrowhead). The most frequent phenotype is shown. (D) $nmo^{P}/+; ey^{R}/+$ *trans*-heterozygotes display a slightly smaller eye compared to wild type. (E) $nmo^{P}; ey^{R}/+$. The nmo^{P} eye phenotype is not modified by reducing a single copy of ey^{R}. (F) $nmo^{P}; ey^{R}$. The size and periphery of the compound eye are rescued compared to C. A single set of ventral vibrissae is present (arrowhead), as in wild type. Flies are oriented with the anterior left. The same results were obtained using nmo^{DB24}, nmo^{adk1}, and nmo^{adk2}.

Heterozygosity for *eya*^{2} enhances the *nmo* eye phenotype: We next characterized flies mutant for both *eya* and *nmo* to investigate a possible genetic interaction. The *eya*^{2} allele results in specific loss of the compound eye due to complete absence of the type I *eya* transcript in the retinal progenitors (BONINI *et al.* 1993; LEISERSON *et al.* 1998; ZIMMERMAN *et al.* 2000). Flies heterozygous for *eya*^{2} or *nmo* are wild type (not shown), yet we found that heterozygosity for *eya*^{2} modified the *nmo* homozygous mutant phenotype (Figure 5C, arrow). Of these flies, 33.6% (35/104) exhibited ventral defects never observed in *nmo* mutants. Specifically, 7.7% (8/104) of flies displayed a reduction of the ventral eye, accompanied by a small, secondary eye field (arrow in Figure 5C). An additional 6.7% (7/104) of flies exhibited an eye-to-head transformation, indicated by an ectopic ocellus in the antero-ventral eye field (data not shown). The remaining 19.2% (20/104) of flies displayed ectopic ventral machrochaete bristles, usually accompanied by loss of the ventral eye (data not shown). Similar phenotypes were observed using the nmo^{adk1} and nmo^{adk2} alleles, as well as *trans*-heterozygous combinations of the *nmo* alleles (data not shown). The manifestation of ectopic cuticle in the eye field, accompanied by inappropriate dorsal head structures, suggests that Eya and Nmo may normally function together in early patterning of the eye and head fields. Indeed, these ventral eye phenotypes were also observed in nmo^{DB24} and nmo^{adk2} somatic clones induced during second instar in flies heterozygous for *eya*^{2} (data not shown).

***eya*^{2} head defects are suppressed by dose-dependent loss of *nmo*:** The dorsal perimeter of the eye is flanked by the orbital bristles, while the ventral margin displays a stereotypical set of macrochaetes followed by posterior microchaetes, collectively termed the ventral sensory vibrissae (Figure 5A, arrowhead; HAYNIE and BRYANT 1986). *eya*^{2} mutants are eyeless and also display a small head with variably missing ventral vibrissae (Figure 5D, arrowhead). In *eya*^{2}*; nmo*/+ flies, we observed an increase in the number of machrochaete-type vibrissae, indicating a rescue in ventral head patterning (Figure 5E, arrowhead). *eya*^{2};nmo^{DB24} double mutants are pharate lethal; however, rare escapers display an expansion of head cuticle indicated by an increase in distance between the orbital bristles and ventral vibrissae (compare Figure 5, D and line in F).

eya mutants are characterized by complete loss of retinal tissue resulting from hyperproliferation during the second instar, followed by massive programmed cell death (PCD) anterior to the MF during third instar (BONINI *et al.* 1993). Activation of apoptosis in *eya*^{2} mutants is an indirect result of the early overproliferation defects (PIGNONI *et al.* 1997) and can also be induced by misexpressing *eya* (CLARK *et al.* 2002). The ventral eye discs of *eya*^{2}; nmo^{DB24} double mutants are larger than *eya*^{2} eye discs (Figure 5, H and I, arrowhead), visualized with the sensory organ precursor marker Cut (BLOCHLINGER *et al.* 1990) and the mitotic marker cyclin B (KNOBLICH and LEHNER 1993). Intriguingly, proliferation appears to occur at the same level in *eya*^{2} and *eya*^{2}; nmo^{DB24} discs

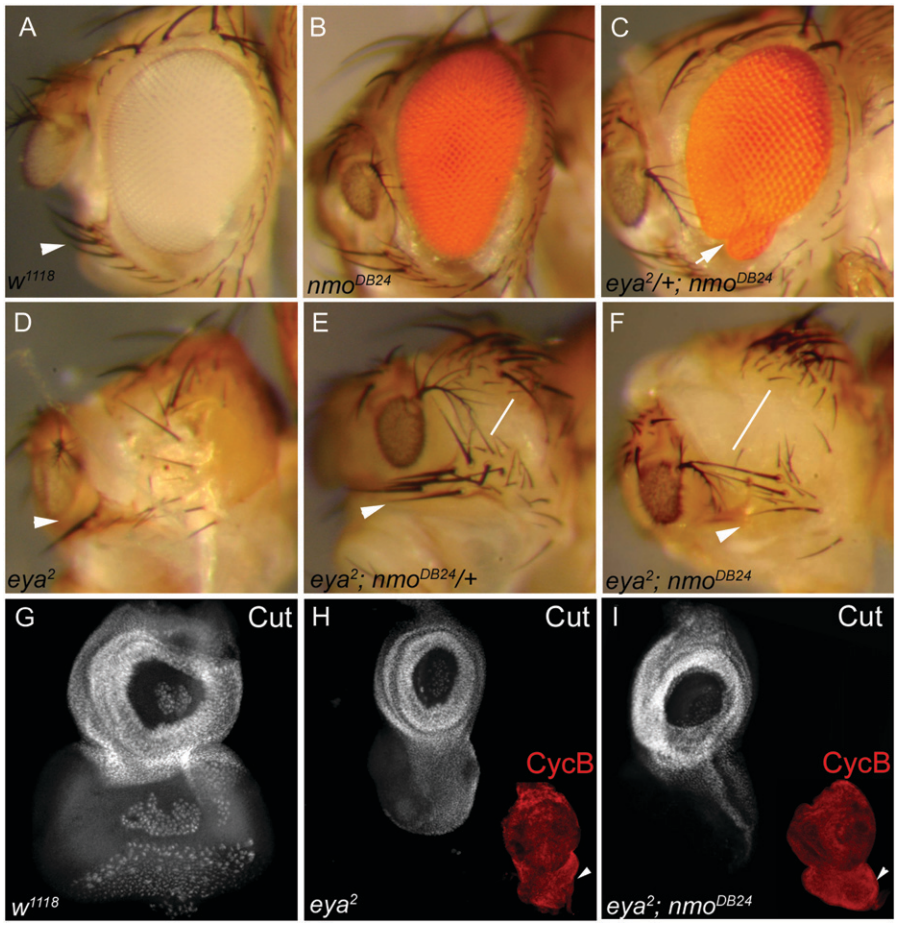

FIGURE 5.—*nmo* and *eya* genetically interact. (A) w^{1118}. Sensory vibrissae surround the ventral eye margin (arrowhead). (B). nmo^{DB24} compound eyes are elongated and narrow. (C) $eya^2/+$; nmo^{DB24}. A secondary eye field develops at the ventral margin (arrow). This phenotype accounts for 22.9% of total observed ventral eye defects (33.6% of flies; $n = 104$). (D) eya^2 mutants lack eyes and are missing ventral vibrissae (arrowhead). As a result of smaller heads, ventral eye bristles converge with dorsal orbital bristles. (E) eya^2; $nmo^{DB24}/+$. More ventral vibrissae are observed (arrowhead; compare with D), and the distance from the dorsal orbital bristles is increased (line). (F) eya^2; nmo^{DB24}. The ventral vibrissae have a nearly wild-type pattern (arrowhead), and their distance from the orbital bristles is further rescued from E (line). (G–I) Imaginal eye discs are oriented with the anterior at the top, dorsal left. White images, anti-Cut; red images in H and I, anti-cyclin B. (G) w^{1118}. Anti-Cut labeling (white) marks the antennal disc and anterior-most eye disc cells, which give rise to head cuticle. Additional posterior staining is observed in the PE and ommatidial clusters. (H) eya^2. The eye disc is largely reduced, relative to the antennal disc. (I) eya^2; nmo^{DB24}. The ventral eye disc is enlarged compared to eya^2 (arrowheads near red images), but proliferation (cyclin B labeling, red) is comparable to eya^2 alone (H).

(Figure 5, H and I, red images), while high levels of apoptosis can be detected in both genotypes with acridine orange staining and with an antibody targeted against activated caspase-3 (not shown).

Loss of *nmo* reduces viability of *dac* mutants: We subsequently investigated whether *nmo* genetically interacts with *dac*, the most downstream component of the RDGN. We tested interactions between all the *nmo* alleles and dac^1 (MARDON *et al.* 1994; SHEN and MARDON 1997; MARTINI *et al.* 2000). dac^1 heterozygotes have no external phenotype. As in our loss-of-function analysis with *ey*, heterozygosity for dac^1 did not modify the *nmo* mutant eye phenotype (not shown). Reducing a single copy of *nmo* in dac^1 mutants induced early larval lethality, precluding our ability to study their potential interaction during eye development. We obtained similar results using the dac^{E462} allele. We also could not recover heterozygous nmo^{DB24} or nmo^{adk1} eye discs in which we had induced dac^{E462} somatic clones. Moreover, *nmo*; *dac* double mutants died as embryos, suggesting a potential interaction for these genes in additional developmental processes that affect viability of the organism.

***nmo* promotes Ey-mediated ectopic eye induction:** Our loss-of-function analyses suggest that Nmo may interact with the eye-specification factors during eye development. However, these results are difficult to interpret, given the intrinsic positive feedback organization of the RD network. As a result, the network can compensate for simultaneous reduction of two or more of its components, leading to unpredictable phenotypes (CHEN *et al.* 1997; PIGNONI *et al.* 1997). Moreover, *ey*, *so*, *eya*, and *dac* mutants lack eyes due to hyperactivation of PCD, an indirect result of early overproliferation and patterning defects (BONINI *et al.* 1993; CHEYETTE *et al.* 1994; PIGNONI *et al.* 1997; HALDER *et al.* 1998). Thus, the very nature of these mutants impedes classical genetic analysis as the developing eye field is obliterated before retinal specification is initiated. Epistasis between the canonical RD members has consequently been established using targeted misexpression studies that separate the RD factors under consideration from the feedback loop in the eye disc (CHEN *et al.* 1997, 1999; SHEN and MARDON 1997; HALDER *et al.* 1998; PAPPU *et al.* 2003). Therefore, we investigated *nmo*'s potential role in RDGN-mediated eye development using previously established misexpression assays.

A key function of the RDGN is to promote retinal determination. In ectopic eye-induction assays, misexpression of any of the RD factors can deploy the eye-specification program in other tissues, including the

head, wing, leg, thorax, and genitals (Halder *et al.* 1995; Chen *et al.* 1997; Pignoni *et al.* 1997; Shen and Mardon 1997; Bonini *et al.* 1998; Halder *et al.* 1998; Anderson *et al.* 2006; Weasner *et al.* 2007). However, not all cells are able to be respecified to the retinal fate; other endogenous factors, such as Hh and high levels of Dpp, appear to also be required (Pignoni and Zipursky 1997; Halder *et al.* 1998; Chen *et al.* 1999; Kango-Singh *et al.* 2003; Pappu *et al.* 2003). In these assays, Ey is the most potent inducer of ectopic eyes, causing dramatic induction of organized ommatidial clusters on the ventral head, antennae, leg, and wing (Halder *et al.* 1995, 1998; Pignoni *et al.* 1997; Chen *et al.* 1999; Anderson *et al.* 2006). We noted that cells able to be respecified as eye cells in the head, wing, and leg frequently correspond to *nmo*-expressing cells (Chen *et al.* 1997, 1999; Shen and Mardon 1997; Bonini *et al.* 1998; Bessa *et al.* 2002; Anderson *et al.* 2006; Weasner *et al.* 2007). Thus, we hypothesized that *nmo* may be a factor that contributes to eye specification at these remote sites, as well as in the normal eye.

To explore a role for *nmo* in retinal induction, we modulated *nmo* levels and assayed the effects on *ey*-mediated ectopic eye induction utilizing the UAS/GAL4 misexpression system (Brand and Perrimon 1993). *dpp-Gal4* drives expression along the posterior and lateral margins of the eye disc and in a ventro-lateral wedge in the antennal disc, which traverses the *nmo* expression pattern in the MF and antennal segments (Figure 6, A and B). In the wing disc, the A–P stripe of *dpp-Gal4* expression bisects *nmo*-expressing cells where it crosses the dorsal and ventral limits of the presumptive wing hinge (Figure 6, C and D). Ey robustly induces eye development in the dorsal wing hinge primordia (Figure 6O), where loss of Hth is concomitantly observed with ectopic expression of Ey targets, including *dac* (Figure 6E, Bessa *et al.* 2002). Nmo is normally co-expressed with Hth in these cells (Figure 6F), suggesting a possible role for *nmo* in mediating ectopic eye development in these cells.

Targeted expression of *ey* using *dpp-Gal4* (*dpp>ey*) induces ectopic eyes on the anterior head, just below the antennae, at a high frequency (Figure 6, K and S). The normal eye field is also reduced at the dorsal and ventral margins compared to wild type (Figure 6H). Previous studies have shown that induction of ectopic eyes by *dpp>ey* is effectively abrogated in *so*, *eya*, or *dac* mutant cells (Bonini *et al.* 1997; Chen *et al.* 1997; Shen and Mardon 1997; Halder *et al.* 1998). Similarly, we tested the requirement for *nmo* in this assay by expressing *dpp>ey* in nmo^{DB24} and nmo^{P} heterozygotes and homozygous mutants. We observed a dose-dependent reduction in both size and frequency of ectopic eyes induced on the head (Figure 6, I, L, M, and S), suggesting that Nmo is a positive component of Ey-mediated retinal induction. Moreover, Nmo also contributes to formation of ectopic eye fields in the wing and leg, as we observed a similar dose-dependent reduction in the size of Ey-induced retinal fields in cells heterozygous or mutant for *nmo* in these tissues (Figure 6, P and Q).

During third instar, *ey* expression is restricted to anterior cells of the eye disc, where one of its functions is to repress furrow progression by inhibiting *eya* expression (Bessa *et al.* 2002). *dpp-Gal4* drives expression at the lateral poles of the MF (Figure 6A; Shen and Mardon 1997). The posterior eye field of *dpp>ey* discs, labeled with an antibody against the nuclear neuronal antigen ELAV (Robinow and White 1991), displays loss of ommatidial clusters from the dorsal and ventral margins and a mild reduction in the size of the eye disc (Figure 6H). In addition, clusters of ectopic ELAV-positive ommatidia are observed in an expanded ventral region of antennal discs (arrowhead in Figure 6H), which give rise to ectopic eyes in the adult (Figure 6K). These cells are fated to give rise to the antero-ventral head cuticle surrounding the eye (Haynie and Bryant 1986). Reducing *nmo* in *dpp>ey* flies caused a further decrease in the number of ELAV-labeled photoreceptors from the dorsal and ventral margins of the normal eye field, in addition to reducing the ectopic eye fields in the antennal disc (Figure 6I) We also observed an overall reduction in the size of the eye-antennal disc (Figure 6I). This manifests as a dose-dependent reduction in the compound eye (Figure 6, P and Q). Taken together, these results suggest that *nmo* promotes eye specification in both normal and misexpression contexts.

We predicted that, if Nmo generally promotes retinal specification, co-expression of *nmo* with *dpp>ey* would result in an expansion of both endogenous and ectopic eye fields. Consistent with this hypothesis, the frequency and size of ectopic retinal fields on the anterior head, wing, and leg increased compared to *dpp>ey* alone (Figure 6, N, R, and S). In *dpp>ey, nmo* eye discs, large patches of ELAV-positive retinal cells were detected in the antennal disc (Figure 6J, arrowhead). In addition, the normal eye field was expanded along the dorsal–ventral axis, resembling wild type (Figure 6J; compare with Figure 6G). *dpp>ey, nmo* adults also displayed a variety of inappropriate tissue outgrowths from the ventral head cuticle (data not shown), indicating that Nmo may have additional roles in cell fate decisions.

Nmo promotes Eya-mediated ectopic eye induction: We further tested the requirement for *nmo* in retinal induction by repeating our misexpression assay using *UAS-eya²*, which encodes the type II *eya* cDNA (Bonini *et al.* 1998). We found that the *UAS-eya²* responder line induced ectopic eyes more potently than *UAS-eya¹*. In agreement with a previous study (Bonini *et al.* 1997), we found that *dpp>eya²* produced infrequent small patches of ectopic eyes on the ventral head and only very rare cases of retinal development on the wing and leg when reared at 25° (data not shown). To determine if *nmo* also promotes Eya-mediated eye formation, we repeated our

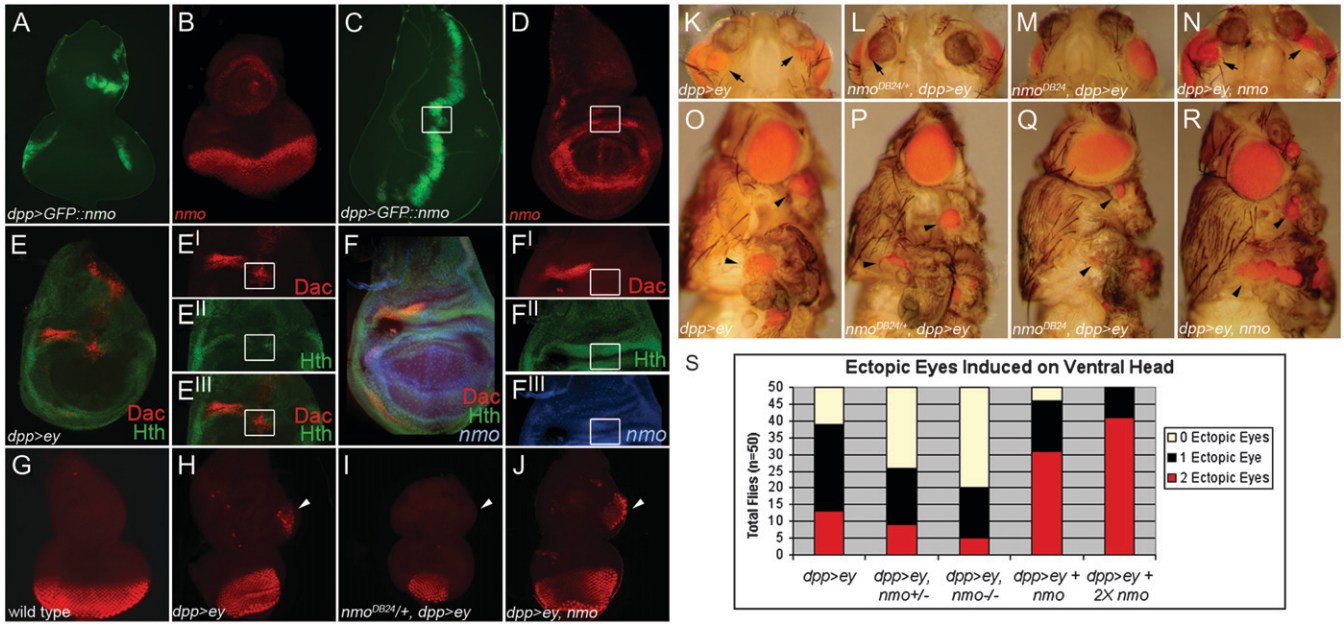

Figure 6.—*nmo* potentiates Ey-mediated ectopic eye induction. (A and C) *UAS-GFP::nmo/+*; *dpp-Gal4/+* (green). (B and D) *nmo-lacZ* (red). (A and B) *dpp-Gal4* (green) targets expression in the dorsal and ventral poles of the eye disc and in a ventral wedge in the antennal eye disc, which bisects *nmo*-expressing cells (red, B). (C and D) *dpp-Gal4* (green) drives expression along the A–P boundary of the wing disc, which intersects with *nmo* expression (red) at the dorsal wing hinge (boxes). (E) *UAS-ey/+*; *dpp-Gal4/+* wing disc. E′–E‴ is an enlarged view of the dorsal wing pouch in E. Ectopic eyes are induced in cells ectopically expressing Dac (red, E′) and with reduced Hth (green, E″). E‴ is a composite of E′ and E″. (F) *nmo-lacZ* (blue) wing disc, Dac (red), and Hth (green). F′–F‴ is an enlarged view of the dorsal wing pouch in F. Dac is not normally expressed in the dorsal wing hinge (F′; compare with E′), although Hth (F″) and *nmo* (F‴) are normally co-expressed in dorsal wing cells able to be respecified to the eye fate (boxes in C–F). (G–J) Eye discs stained for ELAV (red). (G) w^{1118}. ELAV is normally expressed in the posterior photoreceptors and is absent in the antennal disc. (H) *UAS-ey/+*; *dpp-Gal4/+*. ELAV-positive ectopic photoreceptors are detected in the ventral antennal disc (arrowhead). Photoreceptors do not differentiate at the dorsal and ventral boundaries of the eye field, where Dpp targets expression (see A), and the size of the eye disc is reduced compared to the antennal disc. (I) *UAS-ey/+*; nmo^{DB24}*/dppGal4*. Ectopic photoreceptors are no longer detected in the antennal disc (arrowhead). The normal photoreceptor field, as well as the overall size of the eye/antennal disc, is further reduced compared to H. (J) *UAS-ey/ UAS-nmo*; *dpp-Gal4/+*. Large groups of ectopic photoreceptors are detected in the ventral antennal disc (arrowhead). The normal eye field is rescued (compare with H). (K and O) *UAS-ey/+*; *dpp-Gal4/+*. Ectopic eyes are induced ventrally to the antennae (arrows, K) and on the legs and wing hinge (arrowheads, O). (L and P) *UAS-ey/+*; *dpp-Gal4/* nmo^{DB24}. Ectopic eyes are induced at a lower frequency and are smaller than in K (arrow, L). Ectopic eye fields on the legs and wing hinge are reduced compared to O. (M and Q) *UAS-ey/+*; *dpp-Gal4*,nmo^{DB24}/nmo^{DB24}. Ectopic eyes are only rarely induced on the head (M). Ectopic eye fields on the leg and wing hinge are considerably reduced (compare with O). The compound eye has the characteristic *nmo* morphology. (N and R) *UAS-ey/ UAS-nmo*; *dpp-Gal4/+*. The size of ectopic eyes induced on the head (N) and on the leg and wing hinge (R) are larger than in K and O, respectively. (S) Quantification of the phenotypes in K–N. The relative frequencies of zero, one, or two ectopic eyes on head cuticle derived from the antennal disc for the indicated genotypes. Loss or co-expression of *nmo* has a dose-dependent effect on both the frequency and the penetrance of the ectopic eye phenotype. Loss of *nmo* significantly reduces the penetrance of head-to-eye respecification.

assay at 29° to increase the penetrance of the *dpp>eya²* phenotype (Figure 7, A and I). Again we observed a dose-dependent reduction in the size and number of ectopic retinal fields induced in the head (Figure 7, B, C, and I), wing, and leg (Figure 7J) by expressing *dpp>eya²* in *nmo* heterozygotes (Figure 7B) and homozygotes (Figure 7C), respectively. Notably, *nmo* contributes more to Ey-mediated ectopic eye induction (Figure 6S) than in assays with exogenous Eya (Figure 7I) or Dac (Figure 8), suggesting that *nmo* may contribute to Ey-mediated activation of *eya* and *dac* in this context.

Eya contributes to propagation of the MF by promoting *dpp* expression (Pignoni *et al.* 1997; Hazelett *et al.* 1998). In *dpp>eya²* flies, we observed expansion of the furrow along the lateral margins of the eye disc (L. R. Braid, unpublished results), resulting in an enlarged compound eye (Figure 7E, arrowhead). Consistent with our hypothesis that *nmo* promotes normal eye development, reducing *nmo* rescues the overgrowth associated with ectopic *eya* [Figure 7, F (arrowhead) and G]. In fact, Dpp-driven expression of *ey*, *eya²*, or *dac* is unable to significantly modify the *nmo* small-eye phenotype (Figure 6Q; Figure 7H; data not shown), indicating that Nmo may function in processes regulating the size of the eye field downstream or independent of the RDGN.

Ectopic *eya* requires exogenous *ey*, *so*, or *dac* to be a potent inducer of ectopic eyes (Bonini *et al.* 1997; Chen *et al.* 1997; Pignoni *et al.* 1997; Bui *et al.* 2000). Co-expressing *nmo* with *dpp>eya²* also provides this synergy, as it enhances the frequency and size of ectopic retinal

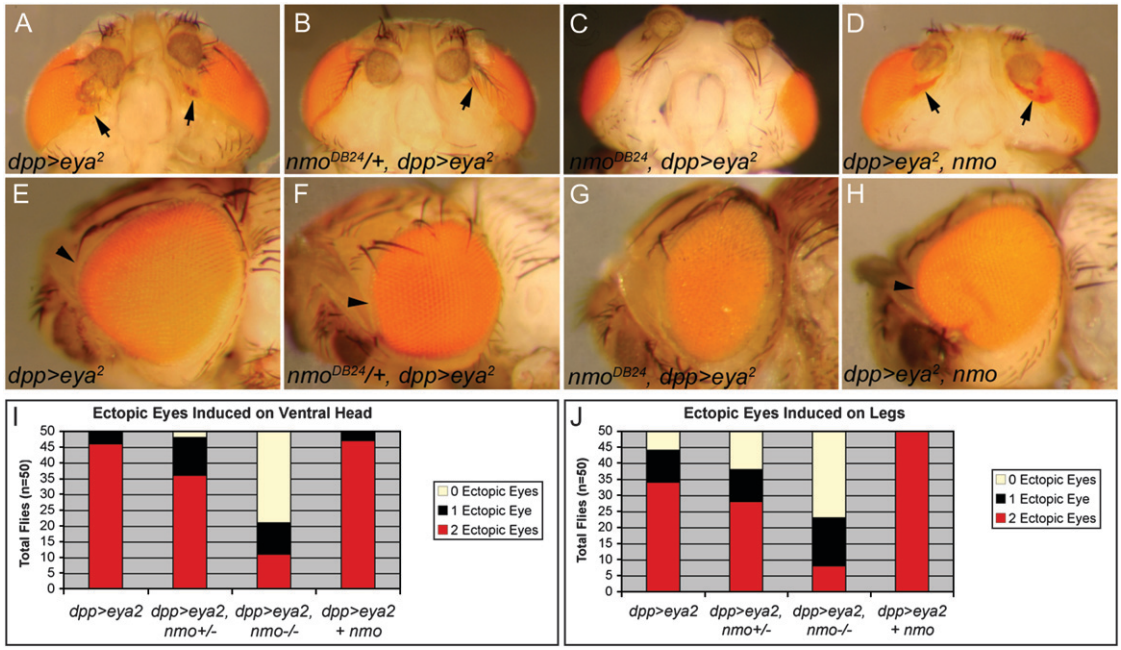

FIGURE 7.—*nmo* potentiates Eya-mediated ectopic eye formation. (A and E) *dppGal4/UAS-eya²*. (A) Small fields of ectopic eyes are induced on head cuticle below the antennae (arrows). (B and F) *nmo^DB24^, dppGal4/UAS-eya²*. (B) Ectopic eye fields are induced less frequently and are smaller than in A (arrow). (C and G) *nmo^DB24^, dppGal4/nmo^DB24^, UAS-eya²*. (C) Ectopic eyes are rarely induced. (D and H). *UAS-nmo/+; dppGal4/UAS-eya²*. (D) Large ectopic eye fields frequently merge with the endogenous eye (arrows). (E) The compound eye is overgrown (arrowhead). (F) The compound eye has minimal overgrowth (arrowhead; compare with E). (G) The compound eye is smaller than wild type and resembles *nmo* mutants. (H) The compound eye is massively overgrown (arrowheads). (I) Quantification of phenotypes in A–D. Loss of *nmo* dose-dependently reduces the frequency of head-to-eye respecification. (J) Quantification of leg-to-eye transformations for the indicated genotypes. As in the head (I), loss of *nmo* dose-dependently reduces the frequency of ectopic eyes induced on the leg. Co-expression with *nmo* increases the penetrance and frequency. Flies were reared at 29°.

fields in the head, wing, and leg (Figure 7, D, I and J). The ectopic eye fields now frequently merge with the compound eye (Figure 7D, arrows), similar to overexpression of *dac* (not shown; CHEN *et al.* 1997; SHEN and MARDON 1997). We also observed further overgrowth of the compound eye compared to *dpp>eya²* alone (Figure 7H, arrowhead), supporting our hypothesis that *nmo* promotes eye formation. Similar synergy is observed in flies co-expressing *nmo* and *dac* (Figure 8).

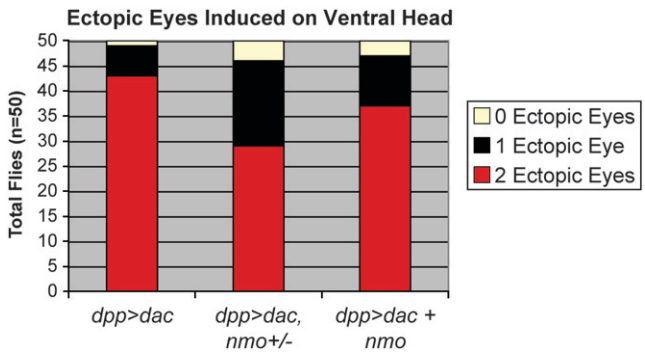

FIGURE 8.—*nmo* potentiates Dac-mediated ectopic eye formation. Quantification of the relative frequency of head-to-eye transformations for the genotypes shown. Heterozygosity for *nmo* reduces the frequency of ectopic eye formation, but less potently than with misexpressed *ey* (Figure 6S) or *eya* (Figure 7I).

***nmo* alone respecifies head precursors as retinal cells:** To further characterize *nmo*'s role in ectopic retinal induction, we expressed *nmo* at high levels using *dpp-GAL4*. Nmo protein levels appear to be tightly regulated, as elevating expression of *UAS-nmo* transgenes has minimal effect on raising total Nmo levels in the cell (FIEHLER and WOLFF 2008; L. R. BRAID, unpublished results). Targeted expression of two copies of *UAS-nmo* with *dpp-Gal4* (*dpp>2Xnmo*) results in mild overgrowth of the dorsal eye (not shown). *dpp>3Xnmo* flies reared at 29° are pharate lethal, although 15% die as early pupae. Consistent with a role in promoting endogenous eye formation, *dpp>3Xnmo* pharate adults display dorsal expansion of the compound eye along the A–P axis (Figure 9B). Dorsal overproliferation can be accompanied by ectopic sensory vibrissae along the ventral eye margin, which is occasionally reduced (data not shown). Notably, 16.7% (28/168) display pigmented, ectopic eyes ventral to the antennae (Figure 9A, arrows). *dpp>3xnmo* pharate adults also have leg, wing, and notum defects (data not shown).

Each ommatidium of the compound eye comprises 20 cells of various types, including neuronal photo-

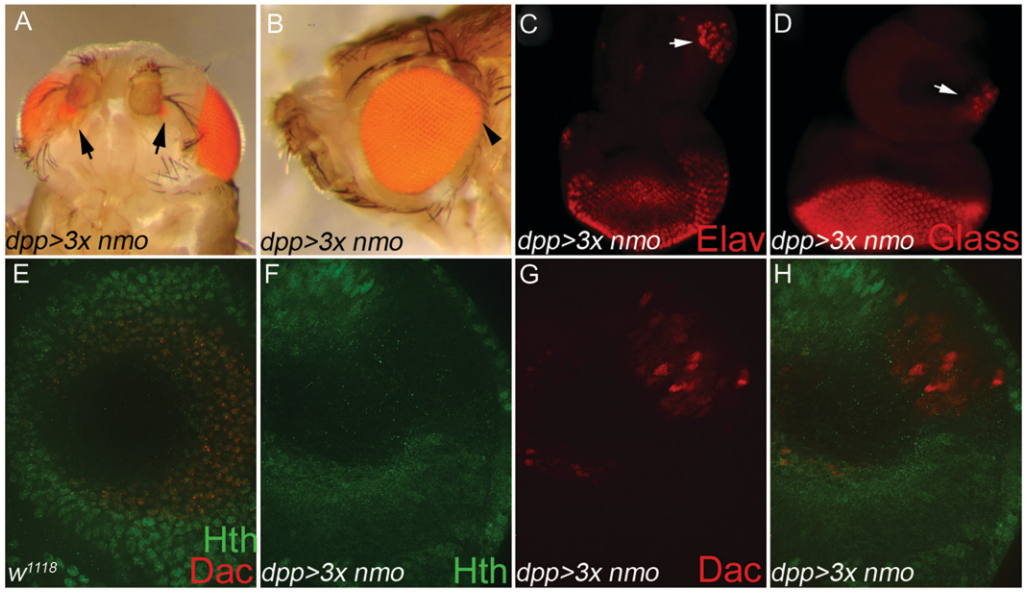

FIGURE 9.—Ectopic Nmo induces head-to-eye respecification in the antennal disc. (A–D and F–H) *UAS-nmo; dppGal4/UAS-nmo* (A) Of pharate adults, 16.7% (28/168) display pigmented retinal cells on the antero-ventral head cuticle (arrows). (B) The dorsal eye is overgrown (arrowhead). (C–H). Imaginal eye/antennal discs. (C) Clusters of ELAV-positive cells (arrow) are detected in the antero-ventral head primordia in 63.6% (28/44) of antennal discs. ELAV is not normally expressed in the antennal disc. (D) Eye-antennal discs labeled with anti-Glass, which is normally absent from the antennal disc, indicate that ventral antennal cells have adopted a retinal fate (arrow). (E–H) Confocal images of the mid-ventral antennal disc taken at ×40. E is a Z-stack of the entire antennal disc. F–H are single confocal planes. (E) w^{1118}. Expression of Hth (green) and Dac (red) in a wild-type disc. Hth is ubiquitously expressed in cells of the outer antennal segments and overlaps with Dac (red) in the third antennal segment. (F) Misexpressed Nmo induces loss of Hth (G) and concomitant ectopic Dac (red) in the outer antennal ring. Endogenous Dac expression is below this focal plane. (H) Composite of F and G. (C–H) Imaginal discs are oriented anterior up, dorsal left.

receptors and non-neuronal accessory cone and pigment cells (READY *et al.* 1976; TOMLINSON and READY 1987a,b). Non-neuronal pigment cells are apparent in the *dpp>3Xnmo* adult ectopic eye phenotype (Figure 9A, arrows). To confirm the presence of photoreceptors, we analyzed *dpp >3Xnmo* imaginal eye discs using the neural markers ELAV (ROBINOW and WHITE 1991) and Glass (ELLIS *et al.* 1993), which are specific to the visual system. ELAV and Glass antigens are not present in wild-type antennal discs (ROBINOW and WHITE 1991; ELLIS *et al.* 1993). Interestingly, we observed clusters of ELAV- and Glass-expressing cells in the ventral antennal disc of 63.6% (28/44) of examined eye discs, which appeared to be forming ommatidia (Figure 9, C and D, arrow). The transformation of presumptive head cells to a retinal fate is therefore more penetrant than the adult phenotype suggests (16.7%). This discrepancy may be the result of early pupal lethality or undetected fate changes in the pharate adults due to the size of the retinal field or the absence of accompanying pigment cells.

Targeted expression of *ey*, *eya*, or *dac* using *dpp-Gal4* downregulates Hth at sites of ectopic eye induction in the antennal and wing discs (Figure 6E; BESSA *et al.* 2002; L. R. BRAID, unpublished results). Similarly, we observe concomitant loss of Hth and ectopic expression of *dac* (Figure 9, F–H) and *eya* (data not shown) in *dpp>3xnmo* antennal discs. These cells correspond to the antero-ventral head primordia, and co-analysis with ELAV verified that Hth is repressed and *dac* is ectopically expressed in cells transformed to an eye fate (not shown). Consistent with previous studies (ANDERSON *et al.* 2006; WEASNER *et al.* 2007), we found that only a subset of Dac-positive cells are respecified as photoreceptors (data not shown). Nmo's ability to cause transformations to the eye fate does not extend beyond the antennal disc, although Hth is repressed in *dpp>3xnmo* wing discs (data not shown). These data imply that elevated Nmo requires endogenous eye factors to deploy the retinal program.

Nmo promotes eye development independently of RDGN gene activation: Our study shows that *nmo* contributes to normal and ectopic eye development mediated by the RDGN. We observed that loss of *nmo* reduced the ability of Ey, Eya, and Dac to induce ectopic eyes and resulted in smaller compound eyes. We also found that misexpression of *nmo* with *dpp-Gal4* could derepress *dac* and *eya* in head cells, causing their respecification to a retinal fate. Thus, we generated *nmo* somatic clones to examine whether Nmo contributes to eye formation by promoting expression of the RD genes. Surprisingly, we did not observe changes in Ey, Eya, *so-lacZ*, or Dac expression in *nmo* loss-of-function clones (Figure 10, B, D, F and H).

The requirement for Dpp in normal and ectopic retinal induction has been well established (WIERSDORFF *et al.* 1996; CHANUT and HEBERLEIN 1997; DOMINGUEZ and HAFEN 1997; PIGNONI and ZIPURSKY 1997; ROYET and FINKELSTEIN 1997; HALDER *et al.* 1998; CHEN *et al.* 1999; KANGO-SINGH *et al.* 2003). *dpp* expression is promoted by the RDGN downstream of *ey* (CHEN *et al.* 1997; HAZELETT *et al.* 1998), and high levels of Dpp are required to antagonize *wg* and promote furrow progression (WIERSDORFF *et al.* 1996; CHANUT and HEBERLEIN 1997; DOMINGUEZ and HAFEN 1997; PIGNONI

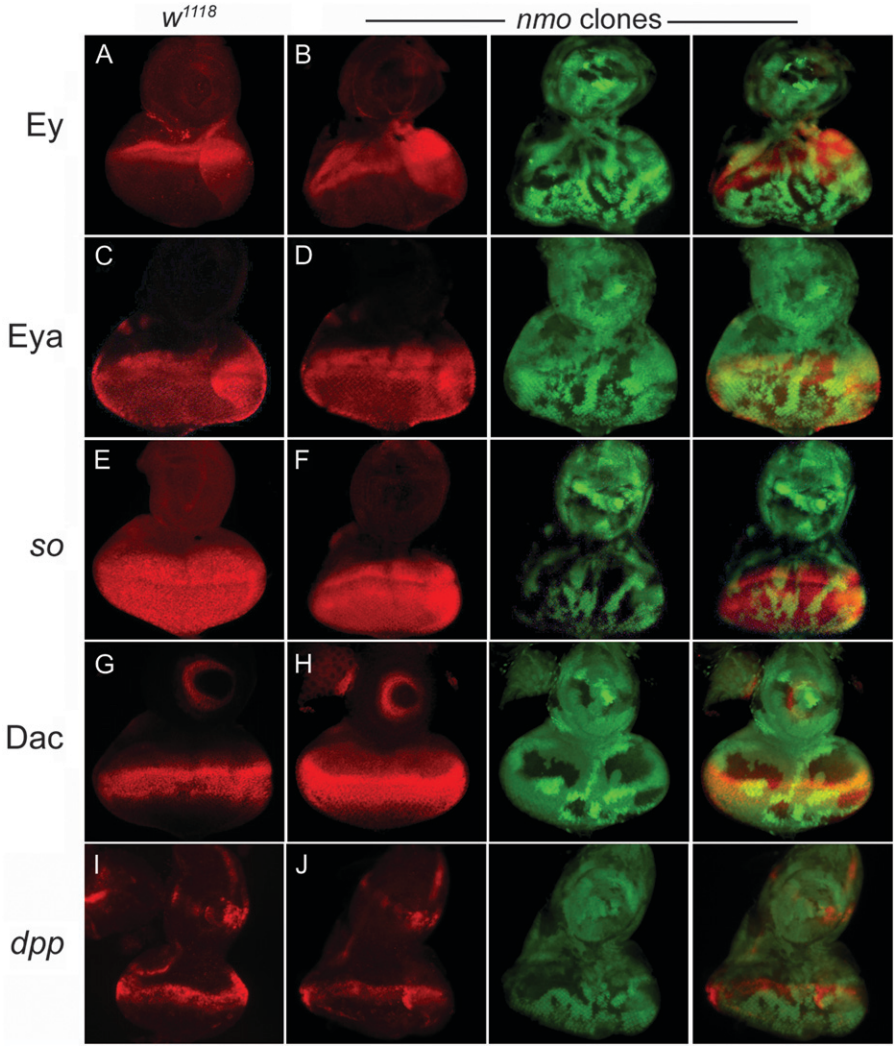

Figure 10.—Nmo promotes eye development independently of RDGN gene activation. (A, C, E, G, and I) Wild type. (B, D, F, H, and J) nmo^{DB24} somatic clones are marked by loss of GFP (green). (C–J) *nmo* loss-of-function clones have no effect on Ey (A and B), Eya (C and D), *so-lacZ* (E and F), Dac (G and H), or *dpp-lacZ* expression (I and J). Eye discs are oriented with the anterior up, dorsal left.

and Zipursky 1997). Therefore, we investigated whether *nmo* promotes eye formation through regulation of *dpp*, using *dpp-lacZ* as a reporter. We found that *dpp* expression was also unchanged in *nmo* somatic clones (Figure 10E), indicating that Nmo promotes eye development without directly modulating RD gene expression or levels of Dpp. Using antibodies against cyclin B and phospho-histone3, we also found that proliferation was unaffected in *nmo* mutant cells (data not shown). These findings suggest that *nmo*'s role in promoting RD-mediated eye development is the result of molecular interactions or the regulation of an as-yet-unidentified common transcriptional target.

***nmo* mediates defects induced by misexpressed *ey*:** Ey deploys the RDGN by initiating expression of *so* and *eya* in the second instar (Halder *et al.* 1998; Kenyon *et al.* 2003) and later complexes with So to activate the neural program in the PPN cells (Zhang *et al.* 2006). However, Ey also complexes with the anterior Wg effectors Tsh and Hth during third instar to delimit the eye/head boundary (Bessa *et al.* 2002). In our ectopic eye induction assays, Nmo promoted eye formation by cooperating with Ey in the ectopic eye field and by antagonizing its activity in the normal eye field. *nmo* and *ey* are co-expressed in the second instar when Ey initiates the RDGN, but are expressed mainly in complementary domains during third instar. Taken together, we hypothesized that Nmo's interactions with Ey may be context dependent.

Since ectopic eye development requires *de novo* deployment of the RDGN, we hypothesized that the positive interaction between Nmo and Ey in this context may represent their interaction in early development, when the eye field is initially specified. Our previous misexpression analysis was performed using *dpp-Gal4*, which drives expression along the posterior and lateral margins of the eye disc in the early instars and in the dorsal and ventral poles of the third instar eye disc. Therefore, we tested this hypothesis using *ey-Gal4*, which is broadly expressed in the eye disc during all three instars.

Directed expression of *UAS-nmo* with *ey-Gal4* (*ey>nmo*) had no effect at 25°, similar to *ey-Gal4* alone (Figure 11, B and C). As previously described, *ey>ey*

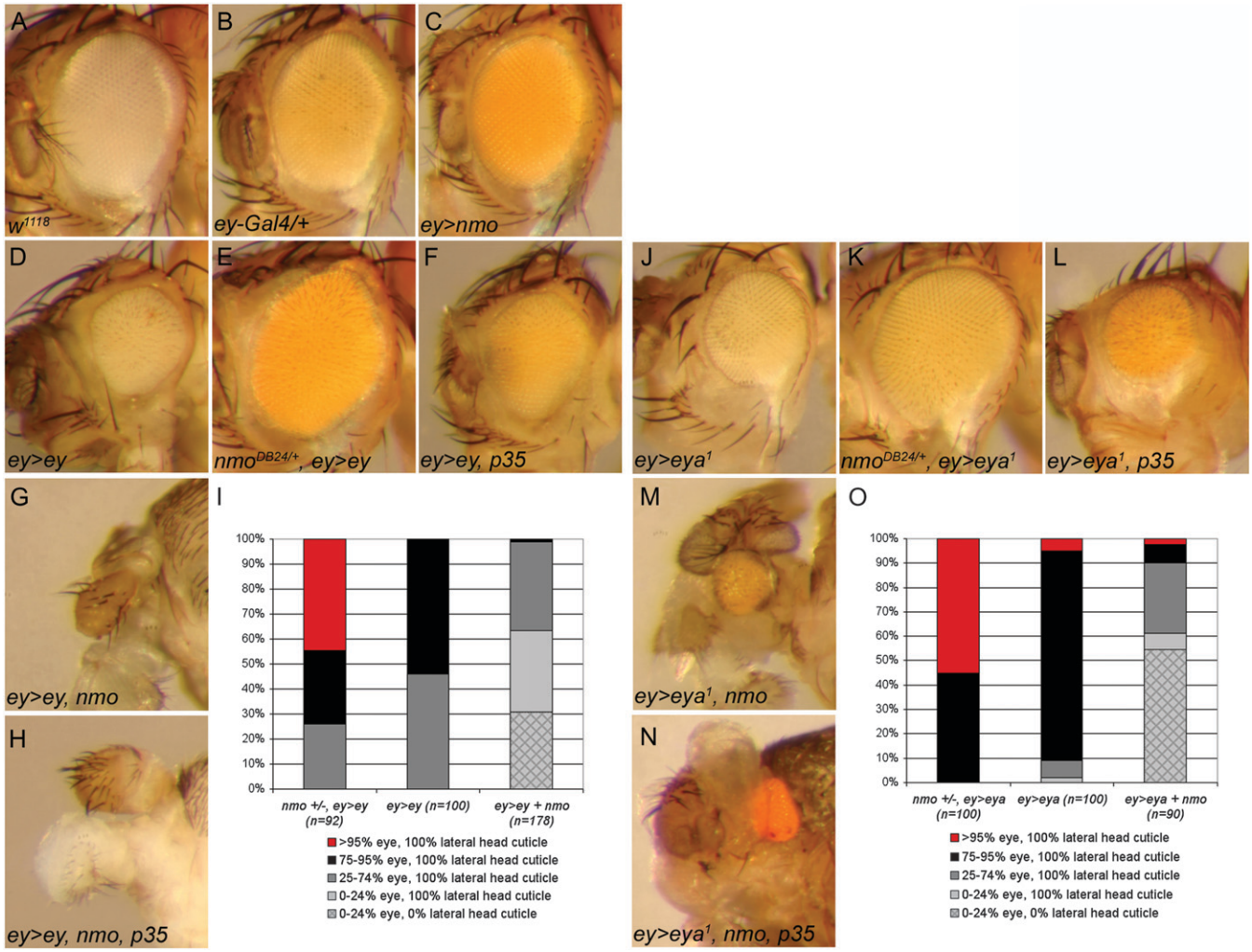

FIGURE 11.—*nmo* promotes early eye defects associated with ectopic *ey* and *eya*. (A) w^{1118}. (B) *ey-Gal4/+* and (C) *ey-Gal4/UAS-nmo* have no detectable external abnormal phenotype. (D) *ey-Gal4/UAS-ey* causes a smaller, rough eye. (E) *ey-Gal4/UAS-ey*; nmo^{DB24}/+. Loss of a single copy of nmo^{DB24} rescues the small eye induced by *UAS-ey* (compare with D). (F) *ey-Gal4/UAS-ey*; $UAS\text{-}p35^{4}$/+. Blocking apoptosis does not phenocopy loss of *nmo* (compare with E). (G) *eyGal4/UAS-ey; UAS-nmo/+*. Flies frequently lack all eye and most head structures. (H) *eyGal4/UAS-ey; UAS-nmo/UAS-p35*. Blocking apoptosis does not modify the defects induced by *UAS-ey* and *UAS-nmo* (compare with G). (I) Quantification of the phenotypes observed in misexpression analysis with *UAS-ey* (D–H). (J) *ey-Gal4/UAS-eya*^{1} results in smaller eyes with dorsal overproliferation. (K) *ey-Gal4/UAS-eya*^{1}; nmo^{DB24}/+. Loss of a single copy of nmo^{DB24} rescues the small eye and dorsal overproliferation induced by *eya* (compare with J). (L) *ey-Gal4/UAS-eya*^{1}; *UAS-p35/+*. Blocking apoptosis does not phenocopy loss of *nmo* (compare with K). (M) *ey-Gal4/UAS-eya*^{1}*; UAS-nmo/+*. Flies display severe reduction of the compound eye and head cuticle. (M) *ey-Gal4/UAS-eya*^{1}*; UAS-nmo/ UAS-p35*. Blocking apoptosis does not modify the defects induced by *UAS-eya*^{1} and *UAS-nmo* (compare with M).(O) Quantification of phenotypes observed in misexpression analysis with *UAS-eya*^{1} (J–N).

induced a complete loss of ventral eye and ommatidial disorganization (Figure 11D; CURTISS and MLODZIK 2000; JIAO *et al.* 2001; PLAZA *et al.* 2001; CURTISS *et al.* 2007). We misexpressed *ey* in heterozygous nmo^{DB24} mutants to test the requirement for *nmo* in the *ey*-induced reduced eye. While nmo^{DB24} heterozygotes appear to be wild type, this background is sufficient to rescue the loss of ventral eye caused by *ey>ey* (Figure 11, E and I)

Loss or ectopic expression of a single RD factor interferes with normal development, presumably by disrupting the delicate stoichiometry of RD factors (CURTISS and MLODZIK 2000; CURTISS *et al.* 2007). This abnormal patterning culminates in high levels of cell death and loss of tissue (SHEN and MARDON 1997; HALDER *et al.* 1998; CURTISS and MLODZIK 2000; JIAO *et al.* 2001; PLAZA *et al.* 2001; CURTISS *et al.* 2007). Since Nmo promotes apoptosis in the pupal eye (MIRKOVIC *et al.* 2002), we tested whether the observed rescue upon reducing *nmo* was an indirect effect of reduced cell death. We reasoned that if eliminating a single copy of *nmo* rescues the *ey>ey* small eye by preventing cell death, then blocking apoptosis in *ey>ey* flies should have a similar effect. Co-expressing the baculovirus caspase inhibitor *p35* (CLEM *et al.* 1991) with *ey>ey* failed to

rescue the small-eye phenotype (Figure 11F), indicating that heterozygosity for *nmo* directly rescues the effects of ectopic *ey* by restoring eye patterning, rather than by modulating cell death. Consistent with Nmo's role in promoting Ey-mediated ectopic eye formation, this finding suggests that *nmo* contributes to Ey function in the early eye field.

Although *ey>nmo* alone had no effect, co-expression of *nmo* greatly exacerbated the developmental defects induced by *ey>ey*. *ey>ey, nmo* animals are pharate lethal and display variable loss of eye and/or head tissue, extending to complete loss of the head and eye, with only the proboscis remaining (Figure 11, G and I). Once again, inhibiting cell death by co-expression of *p35* was unable to modify the phenotype (Figure 11H), suggesting that the observed genetic interactions are the direct result of *nmo*'s effects on Ey-mediated patterning.

***nmo* promotes *eya*-induced eye phenotypes:** We subsequently tested whether Nmo's effects on Ey activity extend to other RD interactions, as *nmo* is also highly co-expressed with *so*, *eya*, and *dac* beginning in the second instar (Figures 2 and 3). Eya is another potent RD factor that can disrupt normal patterning when misexpressed (Bui *et al.* 2000; Hsiao *et al.* 2001). Driving expression of *UAS-eya*^{1}, the type I *eya* transcript (Bonini *et al.* 1997) with *ey-Gal4* caused asymmetric eye defects, with dorsal overproliferation accompanied by loss of the ventral region (Figure 11, J and O). Similar to our genetic analysis with *ey*, we observed that loss of *nmo* rescued the reduced ventral eye induced by *ey>eya*^{1} (Figure 11, K and O), which could not be phenocopied by co-expression of *p35* (Figure 11L). Furthermore, co-expression of *nmo* enhanced the misexpressed *eya*^{1} phenotype, again resulting in gross morphological defects. The retinal field was often still present, although severely reduced and misplaced. Frequently, the majority of head cuticle was absent and malformed although duplicated antennae often remained (Figure 11, M and O). Inhibition of cell death was unable to rescue the *ey>eya*^{1}*, nmo* defects (Figure 11N), indicating that *nmo*'s effects on *ey>eya*^{1} are not the result of modulating activity of the cell death pathway. We also obtained similar results using the *UAS-eya*^{2} transgene (data not shown). Together with our previous analyses, the data imply that Nmo promotes Ey and Eya function during early eye development.

DISCUSSION

In this study we describe novel roles for *nmo* in early eye patterning that are distinct from its known role in planar polarity during late larval development. The RDGN is composed of a highly complex cascade of positive feedback loops (Figure 1A). The fundamental refinement of this delicate system is apparent from the dramatic defects resulting from reducing or ectopically expressing even a single component. Through loss-of-function and misexpression analyses, we provide genetic evidence that *nmo* contributes to patterning events orchestrated by the RDGN during eye development.

Co-expression of the RD genes is spatially and temporally regulated and confers cellular identity through the consequential formation of selector complexes (Figure 1A; reviewed in Pappu and Mardon 2004). For example, So and Eya complex to activate *dac* expression (Chen *et al.* 1999; Jemc and Rebay 2007). Subsequently, Dac can complex with So or Eya to direct expression of complex-specific gene targets (Chen *et al.* 1997; Bui *et al.* 2000). In addition, Ey and So complex to activate *ato* in cells entering the MF (Zhang *et al.* 2006). Repression of *ey* in, and posterior to, the MF limits this interaction to the proneural cells (Pignoni *et al.* 1997; Halder *et al.* 1998). Spatio-temporal regulation of the RD genes is imperative for normal eye and head development, given the deleterious effects of their misexpression on normal eye development (Bui *et al.* 2000; Curtiss and Mlodzik 2000; Hsiao *et al.* 2001; Jiao *et al.* 2001; Curtiss *et al.* 2007). It has been proposed that the availability and relative concentrations of these cofactors affect which protein–protein complexes form (Curtiss and Mlodzik 2000; Curtiss *et al.* 2007). As such, misexpression of the RD genes alters the pool of available cofactors, resulting in mis-specification of cell fate.

Interestingly, reducing any of the eye-specification factors also results in patterning defects, culminating in cell death and loss of tissue (Bonini *et al.* 1993; Cheyette *et al.* 1994; Mardon *et al.* 1994; Quiring *et al.* 1994; Pignoni *et al.* 1997; Halder *et al.* 1998). Thus, reducing an RD factor may be analogous to its misexpression since the relative levels of RD factors are similarly perturbed, leading to abnormal development and hyperactivation of apoptosis. Our data support such a model, since loss of *nmo* restores eye- and head-patterning defects associated with loss of *ey* and *eya*, as it does with early misexpression of these genes. The *ey* and *eya* alleles used in this study are not nulls and therefore may retain some level of activity (Bonini *et al.* 1993; Halder *et al.* 1998). These interactions imply that reducing *nmo* can modulate the transcriptional output of RD complexes, restoring developmental integrity. Moreover, inhibiting apoptosis with co-expression of the caspase-inhibitor *p35* did not phenocopy this rescue, further supporting our hypothesis that Nmo may contribute to eye development by affecting the activity of RD selector complexes rather than by generally promoting cell death.

Although driving *nmo* throughout the eye disc in all stages of development with *ey-Gal4* has minimal effects on its own, and misexpression of *ey* or *eya* causes only small eyes, the combined presence of Nmo and Ey or Nmo and Eya is not compatible with eye and head development. This dramatic synergy, together with the rescue mediated by reducing *nmo*, is consistent with a model in which Nmo affects the function of one or more

of the RD cofactors, thereby affecting the balance of selector factors. We established that Nmo does not regulate Ey, *so*, Eya, or Dac levels in somatic clones, supporting our hypothesis that the observed genetic interactions occur at the protein level. Whether *nmo* is itself regulated by the RDGN is yet to be determined.

The context-specific nature of Nmo's role in mediating RD activity was revealed in our ectopic eye induction assay. Misexpression of *ey* using *dpp-Gal4* not only induced ectopic eyes in the antennal, wing, and leg discs, but also interfered with endogenous eye development. Ectopic *nmo* rescued the dorso-ventral reduction in *dpp>ey* compound eyes, suggesting that Nmo promotes eye development. It further implies that Nmo may differentially affect Ey activity through cell-specific factors, since early co-expression of *nmo* with *ey>ey* had the converse effect, resulting in ablation of the eye and head. Spatial restriction of cofactors to achieve different outcomes is a common developmental strategy. *nmo*'s dynamic pattern of co-expression with Ey, and their complementary expression in the third instar eye and head fields, respectively, supports the hypothesis that Nmo may promote early Ey activity to specify the eye field, while later contributing to patterning of the eye field by antagonizing Ey.

Using ectopic eye induction assays, we investigated Nmo's contribution to eye development in cells expressing exogenous Ey, Eya, and Dac. We demonstrated that endogenous *nmo* potentiates the induction of ectopic eyes in the antennal disc, as well as in the leg and wing. Interestingly, we find that loss of *nmo* restricts the ability of Ey, more than Eya or Dac, to induce ectopic eyes. Ey is most potent inducer of ectopic eyes as it can effectively activate transcription of the downstream RD targets (Halder *et al.* 1995, 1998). Eya, Dac, and So are much less effective in ectopic eye assays (Bonini *et al.* 1997; Chen *et al.* 1997; Pignoni *et al.* 1997; Shen and Mardon 1997; Bui *et al.* 2000; Weasner *et al.* 2007) because their transactivating potential is limited by the number of available RD cofactors (Figure 1A). Thus, we expected that misexpressed *ey* would have the least requirement for *nmo* in the *dpp>ey* assay. This finding suggests that Nmo may contribute to deployment of the RDGN by Ey, since cells with exogenous Eya or Dac more readily compensate for loss of endogenous *nmo* than Ey in the induction of ectopic eyes.

The most convincing evidence for Nmo's role in early eye specification is Nmo's ability to respecify a specific set of head cells as retinal cells when misexpressed alone. Importantly, these are the same subsets of cells able to be transformed by ectopic expression of RD genes (Halder *et al.* 1995; Chen *et al.* 1997; Pignoni *et al.* 1997; Shen and Mardon 1997; Bonini *et al.* 1998; Halder *et al.* 1998; Anderson *et al.* 2006; Weasner *et al.* 2007) and Tsh, which induces *ey* expression (Pan and Rubin 1998). Ectopic eyes induced by other factors such as Optix (Weasner *et al.* 2007) or Eyegone (Eyg) (Jang *et al.* 2003), which promote eye specification through Ey-independent mechanisms, occur in different subsets of cells. We determined that *dac* and *eya* are inappropriately activated in cells transformed by misexpressed *nmo*. It is tempting to speculate that ectopic Nmo perturbs the basal protein–protein interactions that normally repress them, resulting in deployment of the RDGN in the head primordia. Consistent with this model, we observed loss of Hth in cells ectopically expressing *dac*.

The ectopic eye induction assay has been utilized to determine epistasis among the RD factors (Chen *et al.* 1997, 1999; Shen and Mardon 1997; Halder *et al.* 1998; Pappu *et al.* 2003). Although we observed loss of Hth in *dpp>3xnmo* wing discs, this repression does not culminate in activation of any of the retinal genes. This is consistent with our clonal analyses that demonstrate that *nmo* is not required for expression of the RD genes in the eye disc. Moreover, Nmo antagonizes Dpp and Wg signaling in the wing disc (Zeng and Verheyen 2004; Zeng *et al.* 2007), both of which contribute to regulation of *hth* expression in the wing hinge (Azpiazu and Morata 2000). Thus, the observed loss of Hth in *dpp>3xnmo* eye and wing discs may be the result of different mechanisms. For example, elevated Nmo may promote Eya function to repress *hth* (Bessa *et al.* 2002) in the antennal disc. Repression of Hth is not sufficient to deploy the RDGN; therefore Nmo requires the presence of an unidentified factor in the antennal disc to activate eye development.

We showed that *nmo* is not required for expression of Ey, *so*, Eya, or Dac or the secreted morphogen *dpp*. In the eye disc, Wg actively represses *eya*, *so*, and *dac* to antagonize progression of the eye field and promote head development (Baonza and Freeman 2002). We previously showed that *nmo* is an inducible feedback inhibitor of Wg signaling in the wing imaginal disc (Zeng and Verheyen 2004). Although *nmo* expression is not coincident with *wg* in the ME during eye development, we wanted to verify that the observed genetic interactions between Nmo and the RDGN were not due to repression of Wg signaling. Using mutant clonal analysis, we confirmed that, as in the wing, Wg levels are unchanged in both somatic and flp-out *nmo* clones. Furthermore, we observed no change in Wg activity as assayed by stabilization of cytoplasmic Arm (L. R. Braid, unpublished results). These observations are consistent with a previous study indicating that *nmo* does not modulate Arm stability in the eye imaginal disc (Freeman and Bienz 2001). It will be interesting to determine what unidentified factors are affected by loss of *nmo*, and how they contribute to patterning of the eye field.

Novel targets and modes of regulating RDGN activity are rapidly emerging. Recent studies have expanded the repertoire of transcriptional targets regulated by specific RD complexes beyond the scope of the RDGN itself (Ostrin *et al.* 2006; Zhang *et al.* 2006; Jemc and Rebay

2007). Moreover, additional proteins have been identified that modify activity of the canonical retinal factors by various mechanisms. For example, Ey acts as a transcriptional activator when bound to So. However, Ey represses the very same target genes when complexed to Tsh and Hth (Bessa *et al.* 2002). Alternatively, the So–Eya interaction is physically inhibited when So is in complex with the transcriptional corepressor Groucho (Gro) (Silver *et al.* 2003). In addition, Distal antenna (Dan) and Distal antenna related (Danr) were recently identified as retinal factors that complex with Ey and Dac to promote retinal specification through activation of *ato* (Curtiss *et al.* 2007). Whether Nmo directly modulates RDGN output through protein–protein interactions that alter the stoichiometry of available RD cofactors—through post-translational modification of their activity by phosphorylation or indirectly by interactions with noncanonical RDGN regulators—is being investigated. Further characterization of the molecular interactions between Nmo and the RD factors will aid in understanding how cells integrate multiple signals to achieve a specific outcome.

We thank Ryan Fiehler, Graeme Mardon, Uwe Waldorf, and the Bloomington Stock Center for fly strains and Lily Y. Jan, Yuh Nung Jan, Richard Mann, Gines Morata, Richard Mann, and Uwe Waldorf for providing antibodies. We also thank Ashraful Anwar for help with dissections and staining, and Nick Harden and Wendy Lee for comments on the manuscript. This research was supported by a grant from the Natural Sciences and Engineering Research Council of Canada.

LITERATURE CITED

Abu-Shaar, M., H. D. Ryoo and R. S. Mann, 1999 Control of the nuclear localization of Extradenticle by competing nuclear import and export signals. Genes Dev. **13:** 935–945.

Anderson, J., C. L. Salzer and J. P. Kumar, 2006 Regulation of the retinal determination gene dachshund in the embryonic head and developing eye of Drosophila. Dev. Biol. **297:** 536–549.

Azpiazu, N., and G. Morata, 2000 Function and regulation of homothorax in the wing imaginal disc of Drosophila. Development **127:** 2685–2693.

Azpiazu, N., and G. Morata, 2002 Distinct functions of homothorax in leg development in Drosophila. Mech. Dev. **119:** 55–67.

Baonza, A., and M. Freeman, 2002 Control of Drosophila eye specification by Wingless signalling. Development **129:** 5313–5322.

Bessa, J., B. Gebelein, F. Pichaud, F. Casares and R. S. Mann, 2002 Combinatorial control of Drosophila eye development by eyeless, homothorax, and teashirt. Genes Dev. **16:** 2415–2427.

Blackman, R. K., M. Sanicola, L. A. Raftery, T. Gillevet and W. M. Gelbart, 1991 An extensive 3′ cis-regulatory region directs the imaginal disk expression of decapentaplegic, a member of the TGF-beta family in Drosophila. Development **111:** 657–666.

Blochlinger, K., R. Bodmer, L. Y. Jan and Y. N. Jan, 1990 Patterns of expression of cut, a protein required for external sensory organ development in wild-type and cut mutant Drosophila embryos. Genes Dev. **4:** 1322–1331.

Bonini, N. M., W. M. Leiserson and S. Benzer, 1993 The eyes absent gene: genetic control of cell survival and differentiation in the developing Drosophila eye. Cell **72:** 379–395.

Bonini, N. M., Q. T. Bui, G. L. Gray-Board and J. M. Warrick, 1997 The Drosophila eyes absent gene directs ectopic eye formation in a pathway conserved between flies and vertebrates. Development **124:** 4819–4826.

Bonini, N. M., W. M. Leiserson and S. Benzer, 1998 Multiple roles of the eyes absent gene in Drosophila. Dev. Biol. **196:** 42–57.

Brand, A., and N. Perrimon, 1993 Targetted gene expression as a means of altering cell fates and generating dominant phenotypes. Development **118:** 401–415.

Bui, Q. T., J. E. Zimmerman, H. Liu and N. M. Bonini, 2000 Molecular analysis of Drosophila eyes absent mutants reveals features of the conserved Eya domain. Genetics **155:** 709–720.

Chanut, F., and U. Heberlein, 1997 Role of decapentaplegic in initiation and progression of the morphogenetic furrow in the developing Drosophila retina. Development **124:** 559–567.

Chen, R., M. Amoui, Z. Zhang and G. Mardon, 1997 Dachshund and eyes absent proteins form a complex and function synergistically to induce ectopic eye development in Drosophila. Cell **91:** 893–903.

Chen, R., G. Halder, Z. Zhang and G. Mardon, 1999 Signaling by the TGF-beta homolog decapentaplegic functions reiteratively within the network of genes controlling retinal cell fate determination in Drosophila. Development **126:** 935–943.

Cheyette, B. N., P. J. Green, K. Martin, H. Garren, V. Hartenstein *et al.*, 1994 The Drosophila sine oculis locus encodes a homeodomain-containing protein required for the development of the entire visual system. Neuron **12:** 977–996.

Choi, K.-W., and S. Benzer, 1994 Rotation of photoreceptor clusters in the developing *Drosophila* eye requires the *nemo* gene. Cell **78:** 125–136.

Clark, S. W., B. E. Fee and J. L. Cleveland, 2002 Misexpression of the eyes absent family triggers the apoptotic program. J. Biol. Chem. **277:** 3560–3567.

Clem, R. J., M. Fechheimer and L. K. Miller, 1991 Prevention of apoptosis by a baculovirus gene during infection of insect cells. Science **254:** 1388–1390.

Curtiss, J., and M. Mlodzik, 2000 Morphogenetic furrow initiation and progression during eye development in Drosophila: the roles of decapentaplegic, hedgehog and eyes absent. Development **127:** 1325–1336.

Curtiss, J., M. Burnett and M. Mlodzik, 2007 Distal antenna and distal antenna-related function in the retinal determination network during eye development in Drosophila. Dev. Biol. **306:** 685–702.

Czerny, T., G. Halder, U. Kloter, A. Souabni, W. J. Gehring *et al.*, 1999 twin of eyeless, a second Pax-6 gene of Drosophila, acts upstream of eyeless in the control of eye development. Mol. Cell **3:** 297–307.

Dominguez, M., and E. Hafen, 1997 Hedgehog directly controls initiation and propagation of retinal differentiation in the Drosophila eye. Genes Dev. **11:** 3254–3264.

Ellis, M. C., E. M. O'Neill and G. M. Rubin, 1993 Expression of Drosophila glass protein and evidence for negative regulation of its activity in non-neuronal cells by another DNA-binding protein. Development **119:** 855–865.

Fiehler, R. W., and T. Wolff, 2008 Nemo is required in a subset of photoreceptors to regulate the speed of ommatidial rotation. Dev. Biol. **313:** 533–544.

Freeman, M., and M. Bienz, 2001 EGF receptor/Rolled MAP kinase signalling protects cells against activated Armadillo in the Drosophila eye. EMBO Rep. **2:** 157–162.

Garcia-Bellido, A., and J. R. Merriam, 1969 Cell lineage of the imaginal discs in Drosophila gynandromorphs. J. Exp. Zool. **170:** 61–75.

Gibson, M. C., and G. Schubiger, 2001 Drosophila peripodial cells: More than meets the eye? BioEssays **23:** 691–697.

Halder, G., P. Callaerts and W. J. Gehring, 1995 Induction of ectopic eyes by targeted expression of the eyeless gene in Drosophila. Science **267:** 1788–1792.

Halder, G., P. Callaerts, S. Flister, U. Walldorf, U. Kloter *et al.*, 1998 Eyeless initiates the expression of both sine oculis and eyes absent during Drosophila compound eye development. Development **125:** 2181–2191.

Hartman, H., and T. L. Hayes, 1971 Scanning electron microscopy of Drosophila. J. Hered. **62:** 41–44.

Haynie, J. L., and P. J. Bryant, 1986 Development of the eye-antenna imaginal disc and morphogenesis of the adult head in Drosophila melanogaster. J. Exp. Zool. **237:** 293–308.

Hazelett, D. J., M. Bourouis, U. Walldorf and J. E. Treisman, 1998 decapentaplegic and wingless are regulated by eyes absent and eyegone and interact to direct the pattern of retinal differentiation in the eye disc. Development **125:** 3741–3751.

Hsiao, F. C., A. Williams, E. L. Davies and I. Rebay, 2001 Eyes absent mediates cross-talk between retinal determination genes and the receptor tyrosine kinase signaling pathway. Dev. Cell **1:** 51–61.

Ishitani, T., J. Ninomiya-Tsuji, S. Nagai, M. Nishita, M. Meneghini *et al.*, 1999 The TAK1-NLK-MAPK-related pathway antagonizes signalling between beta-catenin and transcription factor TCF. Nature **399:** 798–802.

Jang, C. C., J. L. Chao, N. Jones, L. C. Yao, D. A. Bessarab *et al.*, 2003 Two Pax genes, eye gone and eyeless, act cooperatively in promoting Drosophila eye development. Development **130:** 2939–2951.

Jarman, A. P., E. H. Grell, L. Ackerman, L. Y. Jan and Y. N. Jan, 1994 Atonal is the proneural gene for Drosophila photoreceptors. Nature **369:** 398–400.

Jarman, A. P., Y. Sun, L. Y. Jan and Y. N. Jan, 1995 Role of the proneural gene, atonal, in formation of Drosophila chordotonal organs and photoreceptors. Development **121:** 2019–2030.

Jemc, J., and I. Rebay, 2006 Targeting Drosophila eye development. Genome Biol. **7:** 226.

Jemc, J., and I. Rebay, 2007 Identification of transcriptional targets of the dual-function transcription factor/phosphatase eyes absent. Dev. Biol. **310:** 416–429.

Jiao, R., M. Daube, H. Duan, Y. Zou, E. Frei *et al.*, 2001 Headless flies generated by developmental pathway interference. Development **128:** 3307–3319.

Kango-Singh, M., A. Singh and Y. Henry Sun, 2003 Eyeless collaborates with Hedgehog and Decapentaplegic signaling in Drosophila eye induction. Dev. Biol. **256:** 49–60.

Kenyon, K. L., S. S. Ranade, J. Curtiss, M. Mlodzik and F. Pignoni, 2003 Coordinating proliferation and tissue specification to promote regional identity in the Drosophila head. Dev. Cell **5:** 403–414.

Knoblich, J. A., and C. F. Lehner, 1993 Synergistic action of Drosophila cyclins A and B during the G2-M transition. EMBO J. **12:** 65–74.

Leiserson, W. M., S. Benzer and N. M. Bonini, 1998 Dual functions of the Drosophila eyes absent gene in the eye and embryo. Mech. Dev. **73:** 193–202.

Mardon, G., N. M. Solomon and G. M. Rubin, 1994 dachshund encodes a nuclear protein required for normal eye and leg development in Drosophila. Development **120:** 3473–3486.

Martini, S. R., G. Roman, S. Meuser, G. Mardon and R. L. Davis, 2000 The retinal determination gene, dachshund, is required for mushroom body cell differentiation. Development **127:** 2663–2672.

Mirkovic, I., K. Charish, S. M. Gorski, K. McKnight and E. M. Verheyen, 2002 Drosophila nemo is an essential gene involved in the regulation of programmed cell death. Mech. Dev. **119:** 9–20.

Ostrin, E. J., Y. Li, K. Hoffman, J. Liu, K. Wang *et al.*, 2006 Genome-wide identification of direct targets of the Drosophila retinal determination protein Eyeless. Genome Res. **16:** 466–476.

Pan, D., and G. M. Rubin, 1998 Targeted expression of teashirt induces ectopic eyes in Drosophila. Proc. Natl. Acad. Sci. USA **95:** 15508–15512.

Pappu, K. S., and G. Mardon, 2004 Genetic control of retinal specification and determination in Drosophila. Int. J. Dev. Biol. **48:** 913–924.

Pappu, K. S., R. Chen, B. W. Middlebrooks, C. Woo, U. Heberlein *et al.*, 2003 Mechanism of hedgehog signaling during Drosophila eye development. Development **130:** 3053–3062.

Pignoni, F., and S. L. Zipursky, 1997 Induction of Drosophila eye development by decapentaplegic. Development **124:** 271–278.

Pignoni, F., B. Hu, K. H. Zavitz, J. Xiao, P. A. Garrity *et al.*, 1997 The eye-specification proteins So and Eya form a complex and regulate multiple steps in Drosophila eye development. Cell **91:** 881–891.

Plaza, S., F. Prince, J. Jaeger, U. Kloter, S. Flister *et al.*, 2001 Molecular basis for the inhibition of Drosophila eye development by Antennapedia. EMBO J. **20:** 802–811.

Quiring, R., U. Walldorf, U. Kloter and W. Gehring, 1994 Homology of the eyless gene of Drosophila to the small eye gene in mice and Aniridia in humans. Science **265:** 785–789.

Rayapureddi, J. P., C. Kattamuri, B. D. Steinmetz, B. J. Frankfort, E. J. Ostrin *et al.*, 2003 Eyes absent represents a class of protein tyrosine phosphatases. Nature **426:** 295–298.

Ready, D. F., T. E. Hanson and S. Benzer, 1976 Development of the Drosophila retina, a neurocrystalline lattice. Dev. Biol. **53:** 217–240.

Robinow, S., and K. White, 1991 Characterization and spatial distribution of the ELAV protein during Drosophila melanogaster development. J. Neurobiol. **22:** 443–461.

Rocheleau, C. E., J. Yasuda, T. H. Shin, R. Lin, H. Sawa *et al.*, 1999 WRM-1 activates the LIT-1 protein kinase to transduce anterior/posterior polarity signals in C. elegans. Cell **97:** 717–726.

Royet, J., and R. Finkelstein, 1997 Establishing primordia in the Drosophila eye-antennal imaginal disc: the roles of decapentaplegic, wingless and hedgehog. Development **124:** 4793–4800.

Shen, W., and G. Mardon, 1997 Ectopic eye development in Drosophila induced by directed dachshund expression. Development **124:** 45–52.

Silver, S. J., and I. Rebay, 2005 Signaling circuitries in development: insights from the retinal determination gene network. Development **132:** 3–13.

Silver, S. J., E. L. Davies, L. Doyon and I. Rebay, 2003 Functional dissection of eyes absent reveals new modes of regulation within the retinal determination gene network. Mol. Cell. Biol. **23:** 5989–5999.

Staehling-Hampton, K., P. D. Jackson, M. J. Clark, A. H. Brand and F. M. Hoffmann, 1994 Specificity of bone morphogenetic protein-related factors: cell fate and gene expression changes in Drosophila embryos induced by decapentaplegic but not 60A. Cell Growth Differ. **5:** 585–593.

Tomlinson, A., and D. Ready, 1987a Cell fate in the *Drosophila* ommatidium. Dev. Biol. **123:** 264–275.

Tomlinson, A., and D. F. Ready, 1987b Neuronal differentiation in the *Drosophila* ommatidium. Dev. Biol. **120:** 366–376.

Tootle, T. L., S. J. Silver, E. L. Davies, V. Newman, R. R. Latek *et al.*, 2003 The transcription factor Eyes absent is a protein tyrosine phosphatase. Nature **426:** 299–302.

Verheyen, E. M., K. J. Purcell, M. E. Fortini and S. Artavanis-Tsakonas, 1996 Analysis of dominant enhancers and suppressors of activated *Notch* in Drosophila. Genetics **144:** 1127–1141.

Verheyen, E. M., I. Mirkovic, S. J. MacLean, C. Langmann, B. C. Andrews *et al.*, 2001 The tissue polarity gene *nemo* carries out multiple roles in patterning during Drosophila development. Mech. Dev. **101:** 119–132.

Weasner, B., C. Salzer and J. P. Kumar, 2007 Sine oculis, a member of the SIX family of transcription factors, directs eye formation. Dev. Biol. **303:** 756–771.

Wiersdorff, V., T. Lecuit, S. M. Cohen and M. Mlodzik, 1996 Mad acts downstream of Dpp receptors, revealing a differential requirement for dpp signaling in initiation and propagation of morphogenesis in the Drosophila eye. Development **122:** 2153–2162.

Xu, T., and G.M. Rubin, 1993 Analysis of genetic mosaics in developing and adult Drosophila tissues. Development **117:** 1223–1237.

Zeng, Y. A., and E. M. Verheyen, 2004 Nemo is an inducible antagonist of Wingless signaling during Drosophila wing development. Development **131:** 2911–2920.

Zeng, Y. A., M. Rahnama, S. Wang, W. Sosu-Sedzorme and E. M. Verheyen, 2007 Drosophila Nemo antagonizes BMP signaling by phosphorylation of Mad and inhibition of its nuclear accumulation. Development **134:** 2061–2071.

Zhang, T., S. Ranade, C. Q. Cai, C. Clouser and F. Pignoni, 2006 Direct control of neurogenesis by selector factors in the fly eye: regulation of atonal by Ey and So. Development **133:** 4881–4889.

Zimmerman, J. E., Q. T. Bui, H. Liu and N. M. Bonini, 2000 Molecular genetic analysis of Drosophila eyes absent mutants reveals an eye enhancer element. Genetics **154:** 237–246.

Communicating editor: W. M. Gelbart